RSC Applied Polymers

Accepted Manuscript

This article can be cited before page numbers have been issued, to do this please use: M. Gallmeyer, Þ. A. H. Baldvinsson and W. Loo, *RSC Appl. Polym.*, 2026, DOI: 10.1039/D6LP00078A.

ROYAL SOCIETY OF CHEMISTRY

rsc.li/RSCApplPolym

View Article Online
DOI: 10.1039/D6LP00078A

Perspective: Ion Transport Mechanisms and the Significance of Glass Transition Temperature in PEO-based Polymer Blend Electrolytes for Next-Generation Li-Batteries

Marissa Gallmeyer[a†], Thorfinnur A. H. Baldvinsson[a†], Whitney S. Loo[a]*

[a] University of Wisconsin-Madison Department of Chemical and Biological Engineering, Madison WI, 53706

[†]These authors contributed equally

*Corresponding author email: wloo@wisc.edu

Abstract

Polymer blend electrolytes have become a promising avenue to enable solid electrolytes for use in lithium metal batteries. Much of the current literature has explored the effect of glass transition temperature (T_g) on the ionic conductivity of various ion-containing polymer blends. The Vogel-Tamman-Fulcher (VTF) equation is often used to describe the temperature-dependence of the ionic conductivity of these systems, as it considers the segmental dynamics of the blend and accounts for the T_g. The reduced conductivity can be calculated using the VTF parameters and describes the ionic conductivity at a set value away from T_g. Therefore, the reduced conductivity can interpret observed differences in ionic conductivity by removing the effects of segmental motion. In this work, we fit previously reported ionic conductivity data for 15 unique systems based on polymer blends to the VTF equation, allowing us to deconvolute the effects of T_g and ion solvation environment on the ionic conductivity. We divide the blends into three distinct groups, (1) poly(ethylene oxide) (PEO)-based blends with lithium perchlorate ($LiClO_4$), (2) PEO-based blends with lithium bis(trifluoromethanesulfonyl)imide (LiTFSI), and (3) PEO-based blends with single-ion containing polymers. We find that the relative balance between ion solvation environment and segmental dynamics is highly dependent on salt chemistry, where ion transport in blends doped with $LiClO_4$ is highly dependent on segmental dynamics while ion solvation environment plays a larger role in those doped with LiTFSI. For blends with ion-containing polymers, a complex balance between the number of charge carriers and segmental motion exists. Overall, while segmental dynamics strongly influence ion transport, our findings reveal that the incorporation of multiple polymers into an electrolyte can enable engineering of the ion solvation environment to improve ion transport.

View Article Online
DOI: 10.1039/D6LP00078A

Introduction

As the world faces an ever-growing energy demand and a desire to shift away from fossil fuels to move towards renewable energy technologies, the need for improved energy storage has also increased. Rechargeable batteries are a critical part not only of consumer goods, including personal devices and electric vehicles, but also for the grid-scale transition to renewable energy, which requires innovative energy storage solutions.[1,2] While lithium-ion batteries (LIBs) are the current system of choice due to their moderate energy density and good cycleability,[3] they are unable to meet long-term energy demands.[4–7] Lithium metal batteries (LMBs) are one promising technology that can offer increased energy density by replacing the conventional graphitic anode with a lithium metal anode.[6,8,9] However, there are many engineering challenges to overcome before widespread adoption of LMBs. The electrolytes currently used in commercial LIBs consist of mixtures of carbonate-based solvents and a lithium salt.[10] While these liquid electrolytes exhibit high ionic conductivities, up to 10^{-2} S/cm at room temperature, they are highly flammable with their flash points at only ~30 °C and are not compatible with lithium metal anodes.[11] Additionally, their weak mechanical properties can lead to dendrite formation, resulting from nonplanar Li deposition and stripping, which can hinder battery performance. If the dendrites extend the length of the electrolyte, they can cause short-circuiting and additional safety hazards.[12–15] Therefore, developing alternative electrolytes that address the shortcomings of conventional liquid electrolytes is required for adoption of next-generation batteries.[6,12–14,16]

Solid-state electrolytes (SSEs) would allow for the implementation of the more energy-dense LMBs due to their increased safety including being nonflammable, enhanced stability and the potential to inhibit dendrite formation.[12,17–19] An ideal SSE requires high ionic conductivity at ambient temperatures, sufficient electrochemical and chemical stability, high mechanical strength, and low cost.[20–22] In general, polymer electrolytes meet many of these requirements, and they are also stable against lithium metal.[23,24] Despite these favorable characteristics, polymer electrolytes have limited ionic conductivity at room temperature, which impedes their adoption.[25,26] In 1973, Wright et al. first reported poly(ethylene oxide)'s (PEO) ability to solvate and conduct potassium and sodium salts,[27] and in 1983, Armand et al. demonstrated PEO's ability to conduct solvated lithium ions.[23] Based on these initial studies, a wide variety of polymer structures have been explored as SSEs including polycarbonates, polyethers, polyesters, perfluoropolyethers, and polysiloxanes.[26,28–31]

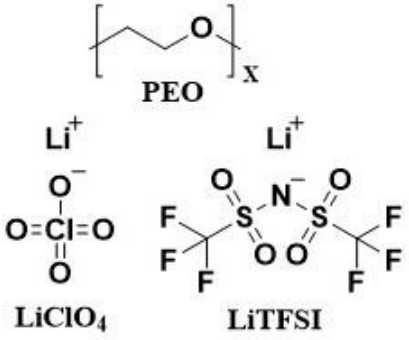

Figure 1. Molecular structures of poly(ethylene oxide) (PEO) and lithium perchlorate ($LiClO_4$), and lithium bis(trifluoromethanesulfonyl)imide (LiTFSI), two of the most commonly used salts in the solid polymer electrolyte space.

View Article Online
DOI: 10.1039/D6LP00078A

PEO doped with various lithium salts has been the primary system of study, with lithium bis(trifluoromethanesulfonyl)imide (LiTFSI) and lithium perchlorate ($LiClO_4$) being the most commonly used salts (**Figure 1**).[21,25] PEO/LiTFSI is considered the benchmark system due to its high ionic conductivity on the order of 10^{-3} S/cm at 90 °C.[32–34] However, the ionic conductivity of PEO/LiTFSI at room temperature is significantly lower, typically around 10^{-4} to 10^{-8} S/cm, due to its semi-crystalline nature.[26,35] To address this limitation and improve the performance of PEO-based electrolytes, many studies have focused on modifying the polymer matrix through polymer blends, copolymerization, or by incorporating additives such as plasticizers and inorganic nanofillers.[36,37] Polymer blend electrolytes (PBEs), where two polymers are blended together, have emerged as promising electrolyte candidates due to the ease and simplicity of preparation and their allowance of good control of physical properties through adjusting blend composition. While PBEs typically consist of miscible blends of two polymers with an added salt, recent studies have focused on blends of neutral and ion-containing polymers, termed single-ion conducting polymer blend electrolytes (SICPBs).[26,38] These studies have shown that PBEs are capable of improved ion transport, allowing for enhanced ionic conductivity and enabling higher cation transference numbers by immobilizing the anion through SICPBs.[26,38] However, the ion transport mechanism in a multicomponent polymer system as well as the thermodynamics governing miscibility in ion-containing polymer blends require further investigation. [25,26,31]

Background

Ion Transport Mechanism in Polymer Electrolytes

Li^+ ion transport in PEO-based electrolytes occurs through Li^+ ion solvation by the ethylene oxide (EO) groups along the polymer chains. The EO groups are polar groups as a result of the electronegativity difference between the carbons and oxygens, and typically, solvation of a single Li^+ ion requires coordination with five to six EOs.[34,39–42] As a result of segmental motion of the polymer, Li^+ ions migrate from one solvation site to another in the presence of an electric field.[43] Therefore, ion transport occurs primarily in the amorphous phase, above the melting temperature (T_m). In the semicrystalline state, the restricted movement of the polymer segments significantly hinders ion transport, and therefore, at temperatures below T_m, the ionic conductivity drops several orders of magnitude due to the reduced amorphous polymer available for ion transport.[36,44–46]

Above the glass transition temperature, T_g, where the polymer subunits undergo segmental motion, ion transport occurs via two mechanisms, vehicular and continuous motion. Vehicular motion is commonly observed in liquid electrolytes and occurs when the coordinating molecules move with the solvated ions. Therefore, in polymer electrolytes, vehicular motion is primarily enabled in low-molecular-weight polymers (i.e., below the entanglement molecular weight, M_e) where single-chain diffusion is possible. At higher molecular weights above M_e, ion transport through continuous motion, either interchain or intrachain, is dominant.[35] Intrachain motion is where an ion moves between solvation sites along the same chain, whereas interchain motion is where an ion moves between solvation sites on different chains. In homopolymer electrolytes with T_g below room temperature, the primary Li^+ ion transport mechanism is continuous motion initiated via the segmental motion of the polymer matrix.[35,43,47] Fast segmental dynamics are enabled above T_g and T_m, while at temperatures below T_g, the motion of the polymer chain is minimal, leading to

View Article Online
DOI: 10.1039/D6LP00078A

greatly reduced ion transport. In this scheme, the temperature dependence of the ionic conductivity, σ, follows the Vogel-Tamman-Fulcher (VTF) equation, an altered Arrhenius equation using T_g as a reference, according to[26,43,44]:

$$\sigma = A\,T^{-1/2}\exp\left(\frac{-E_a}{R(T-T_0)}\right) \quad (1)$$

where A is a pre-exponential factor, E_a is the pseudo activation energy tied to the segmental motion, R is the universal gas constant, and T_0 is the Vogel temperature, defined as 50 °C below the T_g of an electrolyte, i.e., $T_0 = T_g - 50$. The observed non-linear relationship of logarithmic ionic conductivity with inverse temperature reflects the coupling of ion motion with the polymer segmental motion (see **Figure 2**, left side).[34,48] In glassy polymer electrolytes, which exist at temperatures below T_g, there is very limited chain segmental mobility. In these systems, the relationship between ionic conductivity and temperature is often described by the Arrhenius equation[43,48,49]:

$$\sigma = A\exp\left(\frac{-E_a}{RT}\right) \quad (2)$$

Here, E_a refers to an activation energy of ion motion that is not tied to the polymer segmental dynamics, and the other variables (*A, R, T),* have consistent definitions with Eq 1. The linear relationship between the logarithm of ionic conductivity and the inverse of temperature suggests the ion transport is decoupled from the segmental dynamics (see **Figure 2**, right side).[34,50–52] There is increased interest in developing polymer electrolytes that exhibit decoupled ion transport across a wide temperature window especially above the electrolyte's T_g where coupled ion transport is typically observed. This would unlock new material engineering strategies to increase the rates of ion transport that do not involve tuning the segmental motion, which is the current strategy for increasing the ionic conductivity of polymer electrolytes. Walden plot analysis can be used to help quantify the degree of decoupling where high-performing materials would exhibit superionic behavior.[43,53–60]

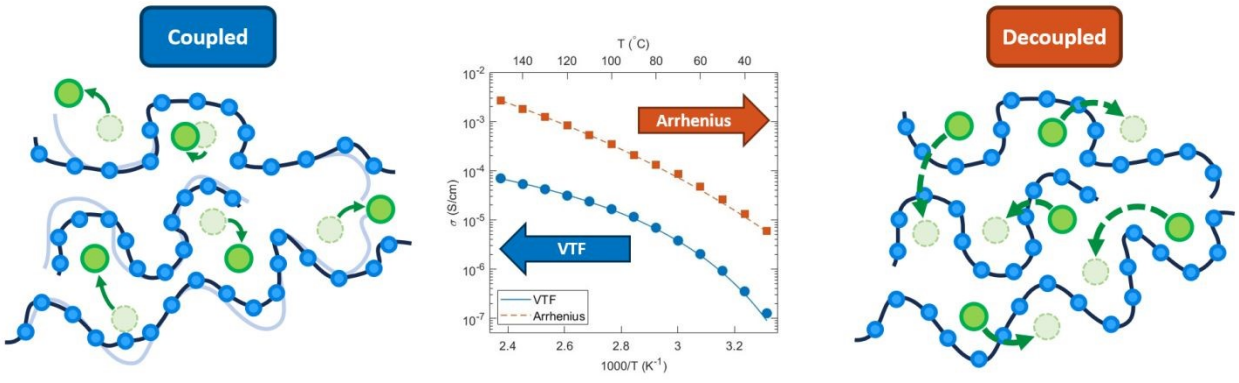

Figure 2. Ion transport mechanisms in systems where ion motion is coupled with segmental motion and those where it is decoupled from the segmental motion.

Several parameters influence the ionic conductivity of polymer electrolytes beyond segmental motion, including ion solvation environment and salt dissociation. The effects of segmental motion

View Article Online
DOI: 10.1039/D6LP00078A

on ionic conductivity can be directly determined by calculating a reduced conductivity, σ_r, using parameters from VTF fits (Eq 1) and is given by:

$$\sigma_r = A\left(T_g + x\right)^{-1/2} \exp\left(\frac{-E_a}{R(x+50)}\right) \quad (3)$$

where x is a given temperature above the T_g. For this study, we consider the ionic conductivity at 100 °C above T_g, i.e., $x = 100$, as this allows us to directly compare the ion transport of various electrolyte systems. However, the choice of x is arbitrary; σ_r may be evaluated at any temperature at which VTF fitting can describe the temperature-dependence of σ. Comparing σ_r values can give insights into the molecular underpinnings for observed differences in the ionic conductivity between polymer electrolytes. For example, we can consider the hypothetical case presented in **Figure 3** comprised of three samples, System A, shown in purple diamonds, System B, shown in red squares, and System C, shown in blue circles. Figure 3a shows the T_g of the three systems, while Figure 3b shows the temperature-dependent ionic conductivity values and fits to VTF behavior, Eq 1, in solid lines. Figure 3c shows the calculated σ_r, Eq 3, of the systems based on the data in Figures 3a and 3b. System A and System B have the same T_g, but a higher T_g than System C. Therefore, System C has faster segmental dynamics than Systems A and B. In Figure 3b, it is shown that System A has the highest ionic conductivity at all temperatures, followed by System C, with System B having the lowest ionic conductivity. However, since σ_r considers the ionic conductivity at a set value above the T_g, new trends emerge in Figure 3c. Therefore, while Systems B and C have different T_g's and ionic conductivities, they have the same reduced conductivity, given by σ_r, indicating that the differences in segmental motion cause the differences in ionic conductivity. Conversely, System A has the same T_g as System B but has a different ionic conductivity and therefore a different σ_r, indicating that other properties, such as variations in the ion solvation environment, are the primary reason for disparities in ionic conductivity. This exercise can be broadly applied to understand the differences in ion transport properties between any electrolytes that display VTF behavior. If little difference is observed in σ_r between two electrolytes, that suggests that segmental motion is the primary factor behind the difference in their ion transport behavior. However, if a significant discrepancy in σ_r is observed, differences in ionic conductivity result from variation in ion solvation environment or salt dissociation rather than segmental motion.[61–63] Deviations in ionic conductivity may also stem from the solvent polarity and favorable interactions between the lithium ions with the polymer solvent and the anion which facilitate a faster transport mechanism and lead to enhanced ion conduction.[64]

View Article Online
DOI: 10.1039/D6LP00078A

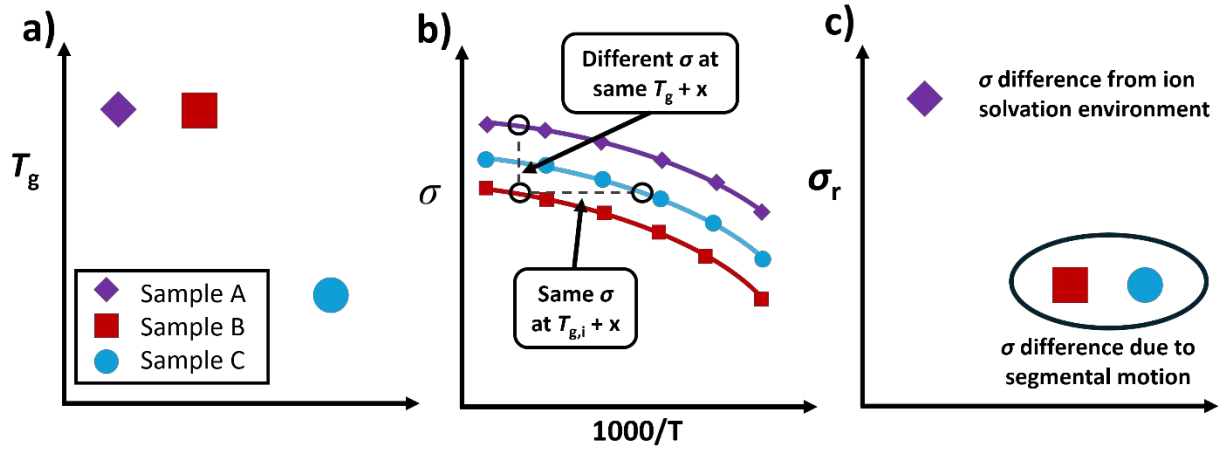

Figure 3. Example of analysis of ion transport mechanism for three polymer electrolytes, Sample A (purple diamond), Sample B (red square), and Sample C (blue circle), where a) shows the T_g, b) shows the temperature dependent conductivity and c) shows the reduced conductivity of the three systems. The x-axis on a) and c) is left blank to indicate comparison with respect to any electrolyte property.

Miscibility and Ion Transport in Polymer Blends

Polymers are large macromolecules making mixing entropically unfavorable.[65] The thermodynamics of binary polymer blends can be described by the Flory-Huggins equation according to:

$$\Delta G_{mix} = k_B T\left\{\frac{\phi_A}{N_A} ln(\phi_A) + \frac{\phi_B}{N_B} ln(\phi_B) + \chi\phi_A\phi_B\right\} \quad (4)$$

where ΔG_{mix} is the Gibbs free energy of mixing, k_B is the Boltzmann constant, T is the temperature, ϕ_i is the volume fraction of component i, N_i characterizes the chain length of component i, and χ is the Flory-Huggins interaction parameter, which quantifies the enthalpic interactions between the distinct monomer subunits, A and B.[66] Therefore, two sufficiently long polymers with large N_i and a negative value of χ will generate a miscible blend, i.e., a single phase system.[67] One method of experimentally probing blend miscibility is through the determination of the glass transition temperature of the polymer blend, $T_{g,blend}$, via differential scanning calorimetry (DSC) or similar methods. It is generally accepted that a singular $T_{g,blend}$ indicates a miscible blend, whereas the presence of two $T_{g,blend}$'s corresponding to each homopolymer component indicates immiscibility, i.e., formation of a two-phase system.[68–70] However, T_g is a bulk property that describes the macroscopic system and the singular value extracted from DSC does not necessarily apply to all of the segments present within the system. For example, in miscible blends of PEO/ poly(methyl methacrylate) (PMMA) that exhibit a single $T_{g,blend}$, it has been shown that the segmental motion of PEO subunits is 12 orders of magnitude faster than that of the PMMA subunits.[71] This behavior can be described by the Lodge-McLeish model, which describes the distinct nanoscale dynamics of two polymer components in a miscible blend. According to this model, each polymer experiences an effective T_g that is determined by the local nanoscale concentration of each polymer component.[72] Therefore, nanoscale heterogeneity can lead to a

View Article Online
DOI: 10.1039/D6LP00078A

broadening of the observed T_g transition in DSC thermograms indicating dynamic nanoscale heterogeneity within miscible polymer blends.[72]

PBEs are ternary systems comprised of two polymers and a salt. In order to maximize ion transport, PBEs must be miscible, as phase separation can result in lower ionic conductivity due to disruptions in ion solvation site connectivity.[73] The introduction of salt impacts the interactions in the system, and typically is accounted for through an effective interaction parameter, $\chi_{eff,}$ which describes the enthalpic interactions between the polymer components in the presence of salt.[70,74,75] Previous work has shown that the miscibility window of two polymers in the presence of salt is typically different from that of the salt-free blends.[70,76,77] The observed changes in blend thermodynamics upon salt addition are highly dependent on the preference for the salt to be solvated by one or more of the polymer components. In the simplest case, only one polymer component is capable of ion solvation, such as PEO/PMMA/LiTFSI where all the ions are solvated by PEO. In these cases, the ion transport mechanism mimics that of PEO homopolymer electrolytes and the presence of PMMA only alters the solvation site connectivity and segmental dynamics of the PEO subunits as described by the Lodge-McLeish model.[78,79] However, both polymers can also participate in ion solvation as is the case with PEO/ poly(1,3,6-trioxocane) (P(2EO-MO))/LiTFSI studied by Gao et al. and PEO/poly(oligo ethylene oxide methacrylate) (POEM)/LiTFSI studied by Gallmeyer et al.[70,80] The ion transport mechanism in these systems is more complicated as there are two distinct rates of ion motion tied to the unique segmental motions of each polymer species.

Single-ion conducting polymer blend electrolytes

In dual ion conductors, where both the cation and the anion are capable of moving, a major fraction of the overall ionic current can be carried by the anions, resulting in a low electrolyte efficiency quantified by the Li^+ transference number (t_{Li^+}).[38,81] In the presence of an electric field, the anions move in the opposite direction of the Li^+ ions. Since there are no reversible electrochemical reactions for the anions at the electrode, the anions accumulate on the electrode-electrolyte interface leading to the formation of concentration gradients, which can cause dendrite growth, reduce the electrochemical stability, and lower the limiting current density.[82–85] Limiting the movement of the anion to generate a single-ion conductor where only the cation can move is one way to increase electrolyte performance. A promising class of SSEs is single-ion conducting polymer electrolytes (SICPEs), introduced by Bannister et al. in 1984, where the anion is covalently bonded to the polymer resulting in high t_{Li^+} values (close to unity). [81,86,87] Compared to PEO-based electrolytes, SICPEs have high T_g's which results in reduced segmental motion negatively affecting Li^+ ion transport. Furthermore, the strong electrostatic interactions between the free cation and bound anion reduce the concentration of free charge carriers, resulting in lower ionic conductivity. [38,58,88,89]

To overcome the inherent trade-off between t_{Li^+} and ionic conductivity, researchers have studied blends of ion-containing polymers (polyanions) and ion-conducting polymers (typically PEO-based), to generate single-ion conducting polymer blends (SICPBs).[90] They demonstrate improved electrochemical performance over single-ion conducting polymer electrolytes, such as superionic transport, as well as increased miscibility.[55,58,60,90] It is worth noting that the blend

View Article Online
DOI: 10.1039/D6LP00078A

thermodynamics in these systems are more complicated than that of the PBEs previously described as only one ion, i.e., the cation, is mobile. The presence of a tethered anion can lead to asymmetric phase diagrams, and modified theories have been developed to define an χ_{eff} that captures the additional interactions present within SICPB systems such as the polymer backbone miscibility, electrostatic interactions, and counterion solvation.[65,91] However, the addition of a rigid, high T_g component, such as a polyanion, reduces the segmental motion and ion transport capabilities of the lower T_g ion-conducting polymer.[72,78] In SICPB systems, the temperature-dependent ionic conductivity often exhibits VTF- or Arrhenius-like behavior. VTF-like behavior is typically observed above the T_g of the system, where the ion motion relies on the free volume generated by segmental relaxations.[43,51] In this case, the mobility of the Li^+ ions is governed by the mobility of the PEO chains. Arrhenius-like behavior is typically observed below the T_g of the system, when the blend is in the glassy state.[92] The mobility of the Li^+ ions is independent of the mobility of the PEO chains.[55,90]

In this perspective, our goal is to determine the effect of segmental motion on the ionic conductivity of various PEO-based PBEs. We have extracted data from 15 distinct PBEs and analyzed their segmental dynamics and ion transport properties. The PBEs are classified into three groups: (1) PEO-based blends with $LiClO_4$, (2) PEO-based blends with LiTFSI, and (3) PEO-based SICPBs. In each section, we evaluate the interactions between the polymer components by fitting available T_g data to known models and calculate σ_r for the PBEs to enable direct comparison of ion transport properties between distinct polymer chemistries. Overall, we find that although polymer segmental motion is a factor across all three groups, the relative balance between ion solvation environment and segmental dynamics is highly dependent on salt chemistry and unique behaviors emerge between the three groups studied. While segmental dynamics strongly influence ion transport in both PBEs and SICPBs, our findings reveal that tunability of polymer blends introduces a pathway to engineer a more-connected ion solvation environment through polymer architecture, anion selection, salt concentration, and blend composition to improve ion transport without the need for increasing segmental dynamics.

Part 1: PEO/P2/LiClO4

First, we will evaluate PEO-based blends with $LiClO_4$, and **Table 1** contains a comprehensive list of the systems analyzed and corresponding blend properties including PEO weight fraction, w_{PEO}, and the molar salt ratio, r, which quantifies salt concentration in these systems. Here we use polymer 2, P2, to denote the second polymer in the blend that has a distinct chemical structure from PEO. We will begin by discussing the segmental dynamics of the blends, as $T_{g,blend}$ can provide insights into the enthalpic interactions between the polymer components and salt. All blends exhibit one T_g and are therefore macroscopically miscible. In order to accurately describe the trends of the T_g's for the PBEs considered in this study, we apply the Kwei equation given by[93]

$$T_{g,blend} = \frac{T_{g,1}w_1 + kT_{g,2}w_2}{w_1 + kw_2} + qw_1w_2 \quad (5)$$

where $T_{g,i}$ is the T_g of component i and w_i is the weight fraction of component i. This equation also contains two fitted parameters, k and q, which describe the expansion volume differences and

View Article Online
DOI: 10.1039/D6LP00078A

interactions between the two polymers, respectively.[94,95] If $k = 1$ and $q = 0$ for a blend, then the expansion volumes are essentially the same between the two polymers and the interactions are neutral. Mathematically, this would reduce the Kwei equation to the Fox equation, which describes ideal mixing. If $k \neq 1$ and $q = 0$, then the steric behaviors of the polymers are different, but the interactions between them are neutral, as described by the Gordon-Taylor equation.[93,94,96,97] Our analysis found that neither the Fox equation nor the Gordon-Taylor equation were able to accurately predict $T_{g,blend}$. This indicates that the interactions in these ternary systems are nonideal and include attractive or repulsive forces that require the quadratic term in the Kwei equation to fully capture their effects.[93]

The Kwei fit was applied to the polymers such that $T_{g,1}$ was that of PEO at the given salt concentration and $T_{g,2}$ was dependent on the system under consideration. In blends where the second polymer is believed to participate in ion solvation and is included in the r value of the blends, $T_{g,2}$ is the T_g of the second polymer at the given salt concentration. This can be described by

$$r = \frac{[Li^+]}{[EO_{PEO}+EO_{P2}]} \quad (6)$$

with one exception. In the PEO/ polyethylenimine (PEI)/$LiClO_4$ blends studied by Tanaka et al., the ethylenimine unit is believed to solvate Li very similarly to an EO unit and so the total EO units is a $[EO_{PEO} + EI_{PEI}]$.[98] In blends where the second polymer is not believed to be participating in ion solvation, $T_{g,2}$ in Eq 5 is the T_g of that polymer without salt. The full Kwei fits for the blends are provided in the Supporting Information. In the blends containing PEO and $LiClO_4$, we have found that all of the values of q are negative (see Table 1), indicating that the excess stabilization energy of the backbones is negative and exhibits some degree of packing frustration and unfavorable interactions.[94,99] It is worth noting that the blends with the least negative values, such as PEO/poly(oligo[oxyethylene]oxysebacoyl) (PES), have similar repeat unit structures, while those with more negative values, such as PEO/poly(2-vinylpyridine) (P2VP) and PEO/poly(4-vinylpyridine) (P4VP) contain two polymers with very different repeat unit structures. This further supports the notion that the more negative q values indicate an increased nanoscale phase separation due to structural differences and less favorable mixing energetics and may explain differences in resulting blend properties.[99]

View Article Online
DOI: 10.1039/D6LP00078A

Table 1. The polymer structures and blend properties including salt concentration (r), glass transition temperature (T_g)[a], and Kwei fitting parameters, for PEO/P2/$LiClO_4$ polymer blend electrolytes.

Polymer 2 (P2)	$M_{n,PEO}$ (kDa)	$M_{n,P2}$ (kDa)	w_{PEO}	r	$T_{g,blend}$ (°C)	k	q	ref
PES 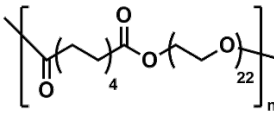	5x10³	1	0	0.1[b]	-31.9	1.00	-2.83	Kim et al.[100]
			0.2		-30.8			
			0.4		-30.3			
			0.6		-28.4			
			0.8		-26.1			
			1		-24.9			
			0.4	0.01[b]	-48.7	-	-	
			0.4	0.02[b]	-47			
			0.4	0.05[b]	-41.4			
			0.4	0.2[b]	-23.9			
PMMA 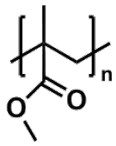	100	120	0.5	0.1	-41	0.122	-126.6	Ghelichi et al.[101]
PEI 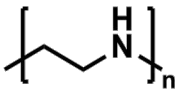	70 & 10³ [c]	87	0.8	0.1[b]	-37.5	1.780	-128.36	Tanaka et al.[98]
				0.07[b]	-30.1	-	-	
				0.14[b]	-40.7	-	-	
				0.25[b]	-41.7	-	-	
P4VP 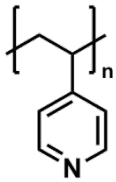	600	50	0.75	0.1	-23	4.767	-558.3	Li & Khan[102]
				0.125	-17	-	-	
				0.167	-29	-	-	
				0.25	-23	-	-	
P2VP 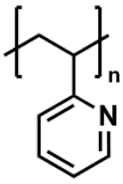	600	200	0.85	0.1	-27	6.478	-555.7	Li & Khan[102]
				0.04	-41	-	-	
				0.05	-39	-	-	
				0.07	-39	-	-	
				0.2	4	-	-	

[a] *All* T_g *values were reported from DSC measurements.*

[b] *Indicates that both polymers participate in ion solvation and are included in the r calculations*

[c] *Ionic conductivity was reported for both molecular weights, but only one set of thermal analysis was provided and so it is assumed that* T_g *is independent of molecular weight and applied to both VTF fits*

View Article Online
DOI: 10.1039/D6LP00078A

A comprehensive study of the PEO/PES/$LiClO_4$ was done by Kim and coworkers and can serve as a case study on the effect of blend properties on the ion transport mechanism.[100] The repeating structure of PES contains a series of EOs separated by esters, as seen in Table 1. Therefore, both PEO and PES contribute to the ion solvation, and r is the ratio of Li to total EO's in both polymers. **Figure 4a** shows the temperature-dependent ionic conductivity of PEO/PES/$LiClO_4$ blends with consistent $r = 0.1$ and varying blend compositions, and VTF fits are shown in solid lines. It is clear that at higher temperatures and at higher PES fractions the VTF equation better represents the ion transport behavior. This is due to the semicrystalline behavior of PEO/$LiClO_4$.[100] At $r = 0.1$, PEO/$LiClO_4$ exhibits a precipitous drop in ionic conductivity corresponding to its T_m at 52.1 °C. In this system, the ionic conductivity increases with increasing PES content, with the blend with the highest PES content having the highest ionic conductivity. However, this also corresponds to the blend with fastest segmental dynamics, i.e., the lowest $T_{g,blend}$. Therefore, we calculated σ_r according to Eq 3 in order to determine if this increase in ion transport is solely due to the difference in segmental motion. **Figure 4b** shows the reduced conductivity, σ_r, of the PEO/PES/$LiClO_4$ blends at $r = 0.1$ as a function of EO mole fraction. As previously described, if the segmental motion was the only determining factor that results in differences in ionic conductivity, we would expect this line to be horizontal at a constant value of σ_r. Instead, we find that the two blends with the lowest EO mole fractions are quantitatively similar, but once we exceed an EO mole fraction of 0.95, there is a steep decrease in σ_r. Therefore, at EO mole fractions below 0.95, the differences in blend segmental dynamics lead to differences in ionic conductivity, while at EO mole fractions above 0.95, the differences in ionic conductivity are due to changes in the ion solvation structure. This indicates that the inclusion of the ester and carbon linkage in PES helps in creating a more favorable ion solvation environment for ion hopping that is unique from that of pure PEO, which increases the rate of ion transport.

View Article Online
DOI: 10.1039/D6LP00078A

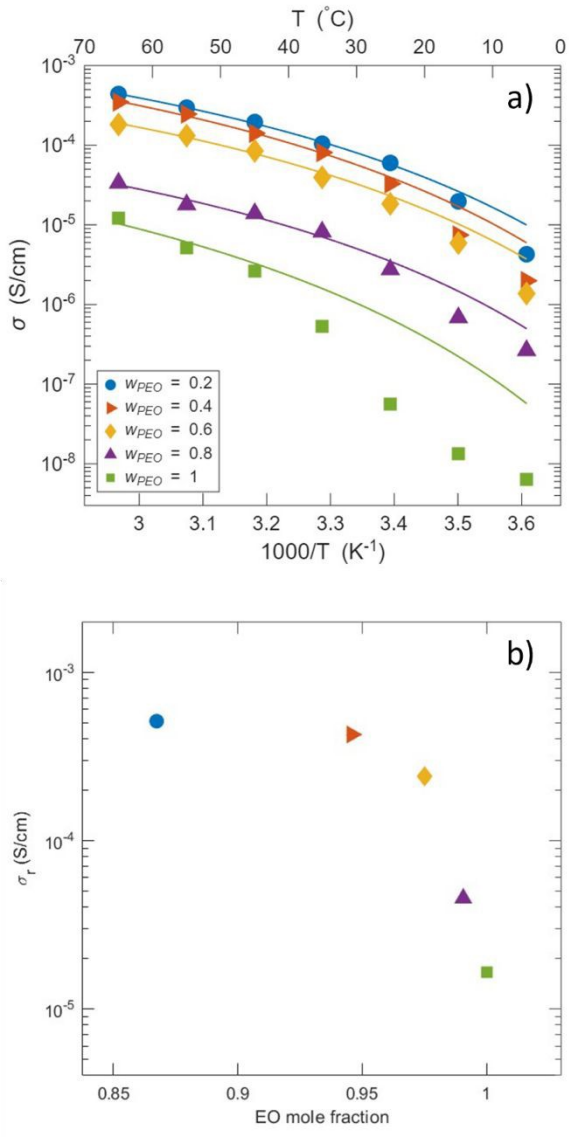

Figure 4. The a) temperature-dependent ionic conductivity where solid lines represent VTF fits and b) reduced conductivity as a function of EO mole fraction of PEO/PES Blends at $r = 0.1$ as studied by Kim et al.[100] σ_r was evaluated at $T = T_g + 100$ for all blends.

It is also important to consider how salt concentration impacts ion transport. **Figure 5a** shows the temperature-dependent conductivity of PEO/PES/$LiClO_4$ at various r values at a constant blend composition of $w_{PEO} = 0.4$. At the highest temperature tested, the ionic conductivity increases with increasing salt content. However, as the temperature decreases, different trends emerge. The blend with the highest salt concentration, $r = 0.2$, undergoes a sharp decrease in ionic conductivity at ~40 °C, while a decrease in ionic conductivity of similar magnitude is observed at ~20 °C for the $r = 0.1$ blend. This decrease in ionic conductivity with decreasing temperature is not observed for the blends with the lowest salt concentrations, $r = 0.01$ and 0.02. Over the salt concentration window studied, the $T_{g,blend}$ spans 25 °C, indicating that the blends have very different rates of segmental motion. To deconvolute the effects of segmental dynamics and salt concentration, we

View Article Online
DOI: 10.1039/D6LP00078A

calculated σ_r from the VTF fitting parameters and plot σ_r as a function of r in **Figure 5b.** All temperatures considered for σ_r fall in the range where the ionic conductivity data can be described by the VTF equation. Here, we see a monotonic increase in σ_r with increasing r, indicating that the difference in ion solvation structure between the blends is the main contributor to the differences in ionic conductivity. As salt concentration increases, the segmental motion of the polymer components decreases due to interactions between the polymer backbone and solvated ions. However, in the PEO/PES/$LiClO_4$ system, the blends with higher salt concentrations are transporting ions faster than what would be indicated by their decreased $T_{g,blend}$ values. These results show that by blending distinct polymers together, one can improve the connectivity of the ion solvation environment at various salt concentrations and enable faster ion transport than what could be achieved by homopolymers alone.

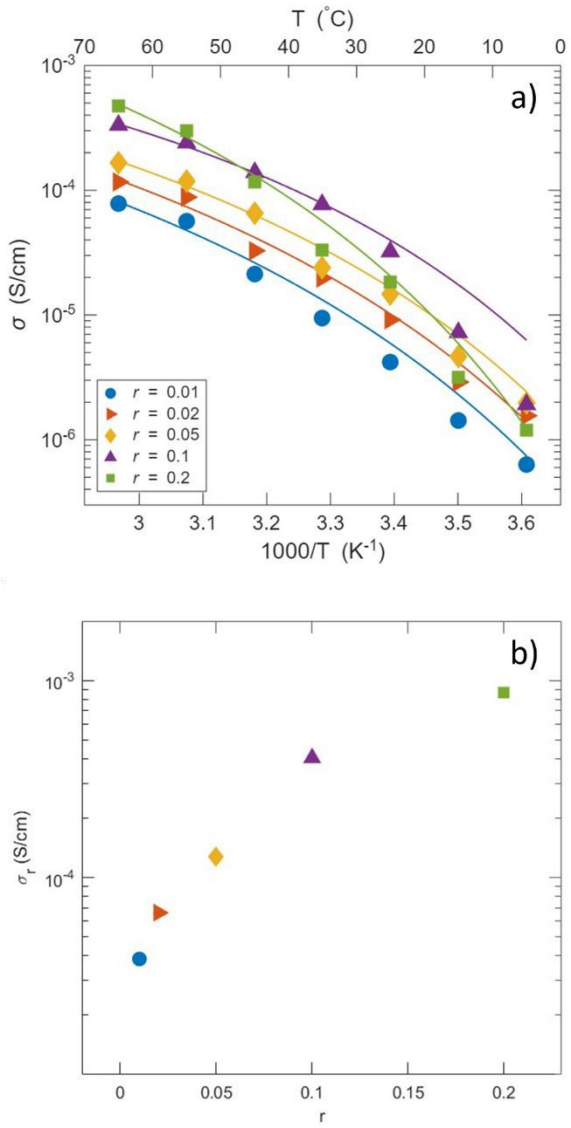

View Article Online
DOI: 10.1039/D6LP00078A

Figure 5. The a) temperature dependent conductivity where solid lines represent VTF fits and b) reduced conductivity as a function of r of PEO/PES Blends at w_{PEO} = 0.4 as studied by Kim et al.[100] σ_r was evaluated at $T = T_g + 100$ for all blends.

A similar analysis was performed on all the blends described in Table 1. **Figure 6a** shows the temperature dependence of the ionic conductivity for all the blends in Table 1 with VTF fits shown in solid lines. For the current and following analysis, the VTF equation was only fitted to the data in the amorphous state of the blends (i.e., at temperatures above reported T_m or crystallization temperature (T_c)); these fits are then extrapolated across the entire temperature range for visualization. The VTF fit applies to all the blends above the melting temperature of PEO, indicating that the blends rely on the segmental motion of the polymers and undergo coupled ion transport. Most of the blends perform poorly at room temperature with ionic conductivities of 10^{-5} S/cm or less as the PEO is semicrystalline under these conditions. As the temperature is increased, the blends show improved ion transport, with the best performers reaching ionic conductivities on the order of 10^{-3} S/cm. The PEO/PEI/$LiClO_4$ blend with an $M_{n,PEO}$ of 70 kDa studied by Tanaka et al. yielded the highest ion conductivities at all temperatures provided. However, it also had a low $T_{g,blend}$ value of -37.5 °C. The PEO/P2VP/$LiClO_4$ blend studied by Li & Kahn, which displayed similar ionic conductivities at high temperatures, had a relatively high $T_{g,blend}$ value of -27 °C. Conversely, the PEO/P4VP/$LiClO_4$ blend in the same study produced some of the lowest ionic conductivities observed in this dataset but had a similar $T_{g,blend}$ of -23 °C. The other blends shown generally fall between or near the PEO/PEI/$LiClO_4$ and PEO/P4VP/$LiClO_4$ blends in both ionic conductivity and $T_{g,blend}$.

Figure 6b shows σ_r as a function of EO mole fraction for the PEO/P2/$LiClO_4$ blends at r = 0.1. The reduced conductivity was calculated at $T > T_m$ for all blends. Overall, the PBEs provided in Table 1 follow the same general trend as the PEO/PES/$LiClO_4$ system. There is a plateau starting at approximately 0.8 EO mole fraction and a sharp decrease at 0.95 EO mole fraction, again indicating that the presence of some non-EO units improves the ion solvation site environment. Additionally, we see that the molecular weight of PEI plays a large role in the ion transport mechanism where the lower molecular weight system, shown in purple triangle, has a lower value of σ_r despite having a higher ionic conductivity than the higher molecular weight system, shown in yellow diamonds. This indicates that changing PEI molecular weight alters the solvation site structure within the PBEs and a higher PEI molecular weight can improve the connectivity between solvation sites. Additionally, the PEO/P4VP/$LiClO_4$ system has the lowest value of σ_r indicating that the P4VP negatively impacts the ion solvation structure within the blend, reducing its efficacy as an electrolyte. In general, it is evident that below 0.95 EO mole fraction, the differences in ionic conductivity are primarily due to differences in segmental motion and not variances in the ion solvation environment, meaning that altering the $T_{g,blend}$ is the most effective way to improve the ion transport within a PBE system doped with $LiClO_4$ at a given salt concentration.

View Article Online
DOI: 10.1039/D6LP00078A

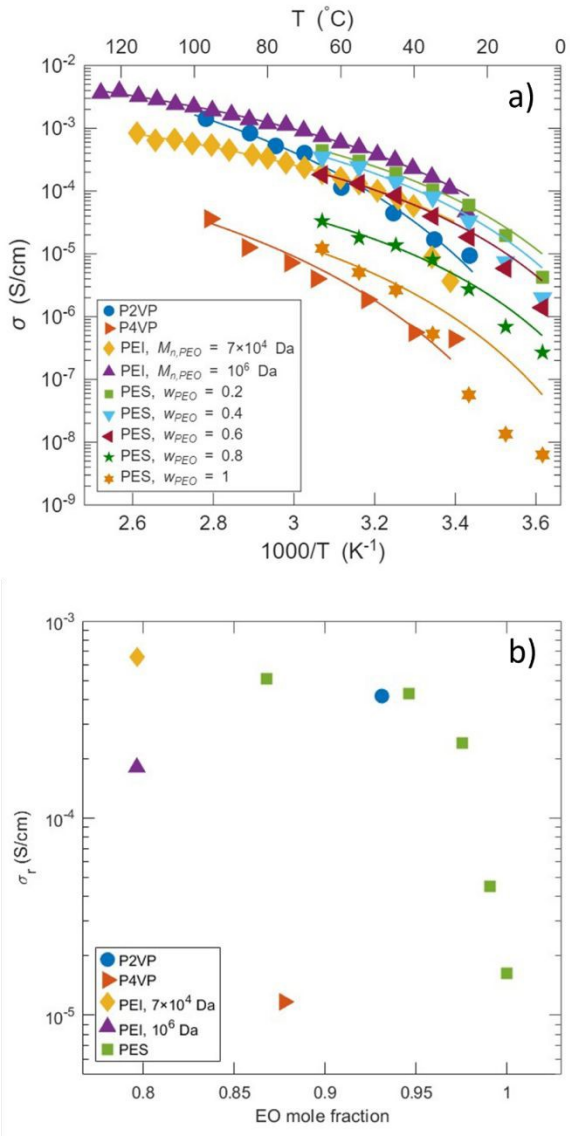

Figure 6. The a) temperature-dependent conductivity where solid lines represent VTF fits and b) reduced conductivity as a function of EO mole fraction for PEO/P2/$LiClO_4$ blends where $r = 0.1$. σ_r was evaluated at $T = T_g + 100$ for all blends.

Part II: PEO/P2/LiTFSI

Recent work on polymer electrolytes has focused on systems containing LiTFSI, as it has been shown to yield the highest ionic conductivities due to its ability to easily dissociate within PEO.[103–105] **Table 2** provides the full catalogue of PEO/P2/LiTFSI blends considered in this study. We applied the same framework as that in Part I, beginning with an analysis of the changes in $T_{g,blend}$. Similar to the blends in Part I, we were unable to predict the $T_{g,blend}$ of the blends with the Fox equation or the Gordon-Taylor equation but found that the Kwei equation provided an accurate representation. The full Kwei fits for the blends are provided in the Supporting Information. The

View Article Online
DOI: 10.1039/D6LP00078A

q values for the PEO/P2/LiTFSI blends were negative but much smaller in magnitude than those in Part I. While this may be due to the variation in molecular structure of the blends, the comparison of the *q* for PEO/PMMA/$LiClO_4$ and PEO/PMMA/LiTFSI blends makes it clear that the molecular structure and electrostatics of the salt affect the enthalpic interactions of the ternary system. Given that $q = 0$ describes a system with ideal interactions, the less negative values in the LiTFSI-containing blends indicate weaker interactions than the $LiClO_4$-containing blends, likely from the weaker bond and easier dissociation of the Li^+ ion.[94,105]

Table 2. Information relating to Polymer blends consisting of PEO and some second polymer with LiTFSI including author, polymer structure, w_{PEO} of the relevant blends, salt concentration, *r*, T_g[a], and Kwei fitting parameters, *k* and *q*.

Polymer 2 (P2)	$M_{n,PEO}$ (kDa)	$M_{n,P2}$ (kDa)	w_{PEO}	*r*	T_g (°C)	*k*	q	ref
PMMA	10	11	0.5	0.05	-40	0.095	-75.42	Sharon et al.
PFPE 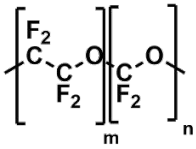	0.4	1	0.2	0.026[b]	-84.0	0.601	-0.0203	Wong et al.[29]
	0.4	1	0.2	0.015[b]	-84.9	0.724	-1.69	
	0.4	1	0.2	0	-85.9	0.350	0.0277	
POEMX 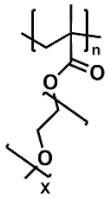 POEM9	30	5.8	0.44	0.1[b]	-39.8	0.0767	-8.671	Gallmeyer et al.[80]
POEM5	30	7.3	0.40	0.1[b]	-35.4	0.406	-20.168	
POEM2	30	8.2	0.31	0.1[b]	-26.51	0.2849	-7.7	
PDTOA 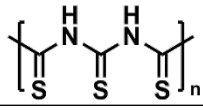	5	6.5	0.5	0.06	21	0.4926	-0.004	Jo et al.

[a] *All* T_g *values were reported from DSC measurements.*
[b] *Indicates that both polymers participate in ion solvation and are included in the r calculations*

The ionic conductivities for the various PEO/P2/LiTFSI blends were extracted and fit to the VTF equation. **Figure 7a** shows the ionic conductivity as a function of inverse temperature for the PEO/P2/LiTFSI systems, with the VTF fits shown in solid lines. As in the previous section, the ability of all blends to be described by the VTF fit indicates that the Li^+ ion motion is coupled to the polymer segmental motion. This is expected as all of the blends contain PEO and have $T_{g,blend}$ values at or below ambient conditions. Using the parameters from the VTF fits, we were able to

View Article Online
DOI: 10.1039/D6LP00078A

calculate σ_r, shown in **Figure 7b** as a function of EO mole fraction. Interestingly, while the PEO/perfluoropolyether (PFPE)/LiTFSI, PEO/poly(dithiooxamide) (PDTOA)/LiTFSI, PEO/POEM5/LiTFSI and PEO/POEM9/LiTFSI blends all have quantitatively similar ionic conductivities, their resulting values of σ_r span over one order of magnitude indicating that the differences in ion solvation environment between the blends lead to the observed differences in ionic conductivity.

Given the varying salt concentrations in the PEO/P2/LiTFSI blends, it is more difficult to draw direct conclusions than in Part I. First, let us address the PEO/PFPE/LiTFSI system shown in blue circles. While this system has a similar ionic conductivity to many of the other LiTFSI containing electrolytes, its salt concentration and polymer molecular weight are low and, therefore, its $T_{g,blend}$ is over 40 ^{o}C lower than any of the other systems. It is not surprising that its σ_r value is lower than most of the other blends shown in Figure 7b as much of its high ionic conductivity is due to the increased segmental motion. The PEO/PMMA/LiTFSI blend, shown in yellow diamonds, has the lowest value of σ_r and ionic conductivity as PMMA does not participate in ion transport and will negatively impact the solvation environment.[78] This is further supported by the three POEM variants, where the PEO/POEM2/LiTFSI system, shown in purple triangles, has a lower ionic conductivity compared to the POEM variants with longer side chains, i.e., POEM5 and POEM9. POEM2 is very similar in structure to PMMA, but with two additional EO units on the side chain. Previous work has shown POEM2 minimally participates in ion solvation and transport in blends with PEO/POEM2/LiTFSI blends.[80] The quality of the solvation environment is complex and cannot be solely correlated with increasing EO fraction or salt concentration. This is made clear by the high value of σ_r of the PEO/PDTOA/LiTFSI system, which has a lower salt concentration than the PEO/POEMX/LiTFSI blends, but has a noticeably higher σ_r at similar EO mole fractions. So, while reducing T_g is a consistent way to improve the ionic conductivity, the variance in σ_r calculated for the PEO/P2/LiTFSI systems demonstrates that there may be additional ways to improve the solvation environment to increase ion transport that are independent of T_g. However, due to the limited body of work in this area, more research is necessary to understand the extent to which this is possible.

View Article Online
DOI: 10.1039/D6LP00078A

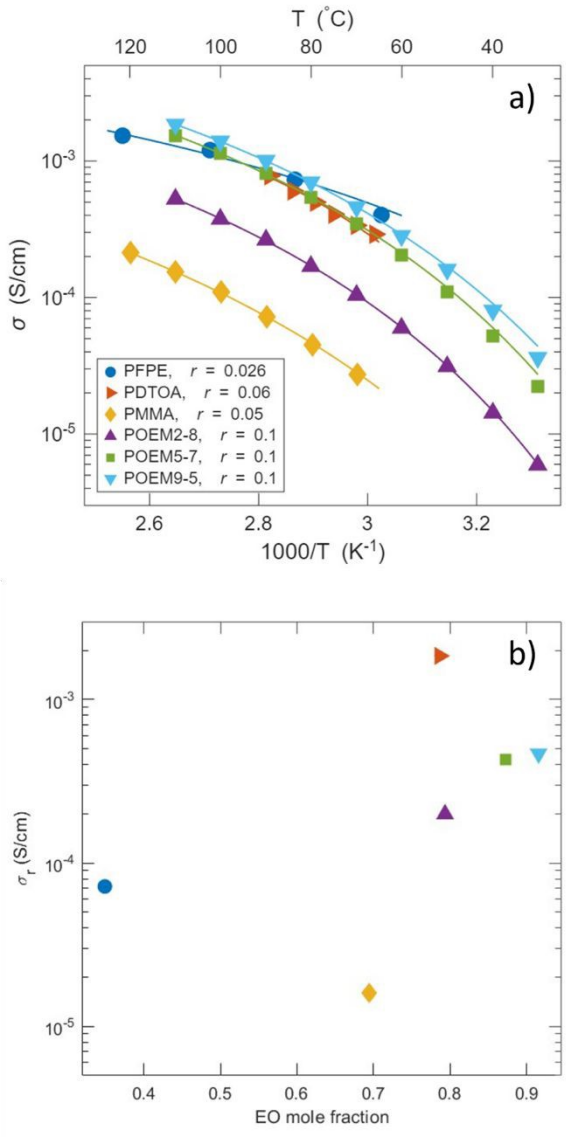

Figure 7. The a) temperature-dependent conductivity where solid lines represent VTF fits and b) reduced conductivity as a function of EO mole fraction for PEO/P2/LiTFSI blends. σ_r was evaluated at $T = T_g + 100$ for all blends.

Part III: Single-ion conducting polymer blend electrolytes

The third class of PBEs analyzed in this study are binary systems consisting of a PEO-based ion-conducting polymer and an ion-containing polymer. The characteristics of the SICPBs considered here can be found in **Table 3**. It's important to emphasize that r is intrinsically linked to blend composition in SICPBs where an increase in r corresponds to an increase in charged polymer concentration. Similarly to the dual ion containing blends, we were able to describe the changes in the $T_{g,blend}$ through the Kwei Equation. The majority of the blends have a k value below 1 with the exception of the PEO/lithium poly[(4-styrenesulfonyl)(trifluoromethyl(S-

View Article Online
DOI: 10.1039/D6LP00078A

trifluoromethylsulfonylimino)sulfonyl)imide] (LiPSsTFSI) blend, which was 1.20. Unlike the dual-ion systems, the q values of the SICPBs span both positive and negative values. This does not agree with Kwei's assertion that a positive q value would lead to a T_g that is higher than the weighted average of the two polymers. Nearly all of the blends display T_g's that are lower than the weighted average, thus indicating that while the Kwei equation can empirically describe equation, the interactions due to the ionic polymers are too complex to be consistently described by the two fitting parameters within the Kwei equation. This likely reflects the physical differences in the interactions between a free and bound salt molecule. It is interesting that the PEO/LiPSsTFSI blend showed $q \approx 0$ and therefore behaves as though there are not any significant interactions and could just as easily be described by the Gordon-Taylor equation. In contrast, the PEO/phenylsulfonyl (trifluoromethylsulfonyl)imide-lithium (P5PhTFSI-Li) blend exhibits the most negative q value, indicating strong nonideal interactions within the system similar to discussed in PEO/P2/$LiClO_4$ systems. While both LiPSsTSFI and P5PhTFSI-Li are based on styrenic monomers, these large differences in q indicate that small changes in polymer backbone or anion chemistry largely influence the non-ideal interactions introduced upon mixing.

Table 3. Information relating to Polymer blends consisting of a single-ion polymer blended with a PEO-based conducting polymer including author, polymer structure, w_{PEO} of the relevant blends, salt concentration, r, T_g[a], and Kwei fitting parameters, k and q.

Polymer 2	*EO Polymer*	$M_{n,1}$ (kDa)	$M_{n,2}$ (kDa)	w_{P1}	r	T_g (°C)	k	q	ref
PLiMTFSI 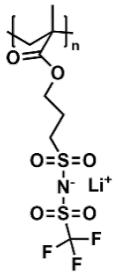	POEM	5.9	25	0.44	0.2	7.23	0.73	-3.13	Yang & Epps[90]
				0.62	0.1	-18.5			
				0.76	0.05	-38.7			
				0.83	0.03	-47.2			
			52	0.44	0.2	19.83	0.55	15.81	
				0.62	0.1	-10.9			
				0.76	0.05	-32.6			
				0.83	0.03	-42.7			
			7	0.44	0.2	-23.0	0.37	5.0	
				0.62	0.1	-39.7			
				0.76	0.05	-52.3			
				0.83	0.03	-53.3			

View Article Online
DOI: 10.1039/D6LP00078A

PLiMTFSI 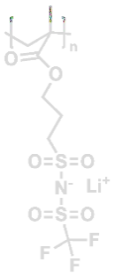	PEO	100	5	0.30	0.298	-6.5	0.19	-1.3	Olmedo Martinez et al.[88]
				0.50	0.128	-30.1			
				0.70	0.055	-41.3			
				0.85	0.022	-45.6			
				0.95	0.006	-50.8			
			50	0.30	0.298	8.0	0.28	18.6	
				0.50	0.128	-15.5			
				0.70	0.055	-33.0			
				0.85	0.022	-43.1			
				0.95	0.006	-48.9			
			>2000	0.30	0.298	20.9	0.35	31.9	
				0.50	0.128	-7.9			
				0.70	0.055	-25.1			
				0.85	0.022	-39.3			
				0.95	0.006	-46.7			
P5PhTFSI-Li 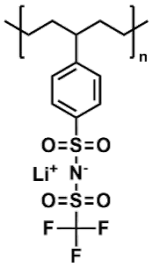	PEO	20	32	0.3	0.29	54.8	0.46	-105.0	Nguyen et al.[106]
				0.5	0.13	2.0			
				0.58	0.087	-17.8			
				0.7	0.051	-35.8			
				0.9	0.013	-42.9			
LiPSsTFSI 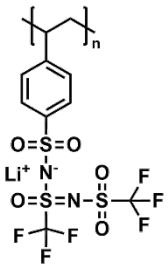	PEO	-	20	0.66	0.05	-15.1	1.20	0.0	Ma et al.

[a]*All* T_g *values were reported from DSC measurements.*

View Article Online
DOI: 10.1039/D6LP00078A

The temperature-dependent ionic conductivity was extracted for all SICPB systems and fit to the VTF equation as well as the Arrhenius equation depending on the nature of the temperature dependence. **Figure 8a** shows the ionic conductivity as a function of inverse temperature at a fixed salt concentration of $r \approx 0.05$, where the VTF fits are indicated by solid lines and Arrhenius fits are indicated by dashed lines. As before, the VTF equation is employed only in the amorphous state ($T > T_m$) but were not extrapolated to the entire temperature range. The onset of Arrhenius behavior in the POEM/poly[lithium sulfonyl (trifluoromethane sulfonyl)imidemethacrylate] (PLiMTFSI) blends aligns with an increase in molecular weight and concentration of PLiMTFSI, while the other systems exhibit VTF behavior. Notably, the POEM/PLiMTFSI-52 blend, which exhibits Arrhenius behavior above T_g, shows the highest ionic conductivity at elevated temperatures, highlighting the potential performance improvements when ion transport is decoupled from segmental motion across a wide temperature range. Overall, the ionic conductivities of the SICPBs are quantitatively similar and only span one order of magnitude at constant temperature. In these systems, the PEO-based polymer is the main contributor to ion solvation and transport, indicating that the chemical structure of the polyanion does not strongly affect ionic conductivity. Therefore, it is likely that blend composition will have a stronger effect on ionic conductivity. **Figure 8b** plots the ionic conductivity at 90 °C as a function of blend composition, r, which is directly correlated to polyanion concentration in SICPBs. For most systems, the maximum ionic conductivity is reached at an intermediate concentration of polyanion, after which the ionic conductivity decreases. While an increase in r correlates to an increase in charge carriers, it also leads to a decrease in blend segmental dynamics as the concentration of high T_g polymer increases. Therefore, this non-monotonic behavior indicates that there is a careful balance between the number of charge carriers, ion solvation structure, and segmental motion that leads to fast ion transport in SICPBs. Interestingly, the only blend with decoupled ion transport at all salt concentrations, POEM/PLiMTFSI-52, exhibits a less significant decrease in ionic conductivity when r increases compared to the blends with coupled ion transport. This indicates that the ion transport properties are less sensitive to blend composition in systems that exhibit decoupled transport.

View Article Online
DOI: 10.1039/D6LP00078A

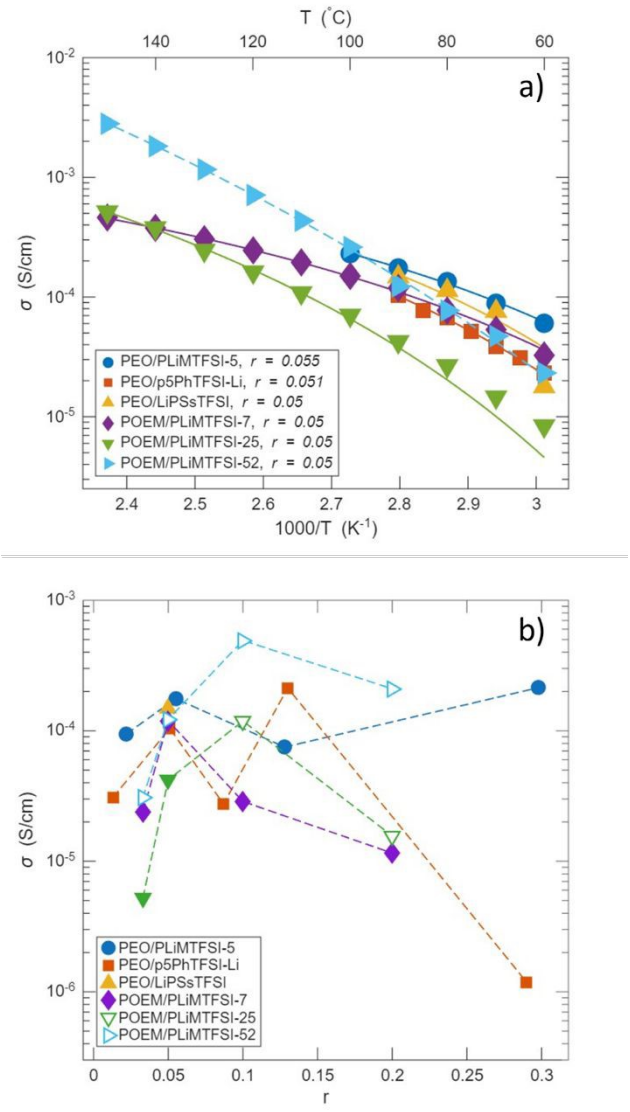

Figure 8. a) Ionic conductivity as a function of inverse temperature at a fixed salt concentration around r = 0.5. VTF fits are shown by solid lines, and Arrhenius fits are shown by dashed lines. **b)** Ionic conductivity as a function of r taken at 90°C for the SICBs. VTF fits are shown by solid symbols, and Arrhenius fits are shown by white filled symbols. Dashed lines are used to connect the data points to guide the eye.

To separate the effects of salt concentration and segmental dynamics, σ_r was calculated as a function of r and is shown in **Figure 9**. It should be noted that the blends that exhibit Arrhenius behavior are not included in this analysis as their ionic conductivity cannot be described by the VTF equation, which is required to calculate σ_r. When σ_r is considered, it becomes clear that segmental motion is not the only contributor to ionic conductivity as the quantitative values of σ_r span several orders of magnitude. In general, the trends with respect to r are similar to those observed in Figure 8 and a maximum value of σ_r is present at an intermediate value of r that is blend dependent. For example, the PEO/P5PhTFSI-Li yields the highest σ_r at r = 0.13 while the peak value for POEM/PLiMTFSI-7 is at r = 0.05. The highest value of the PEO/PLiMTFSI-5 blends is at r = 0.3, however due to the lack of data it is unclear if the σ_r reaches a maximum there

View Article Online
DOI: 10.1039/D6LP00078A

or continues to increase with increasing PLiMTFSI content. The presence of these maxima indicates that the distribution and solvation of the ions is more important than the number of charge carriers present in the system suggesting that an optimal balance between the number of charge carriers, ion solvation structure, and other factors is met at a specific concentration of charged polymer for each species. This is further supported if we consider just the POEM/PLiMTFSI-7 and the PEO/PLiMTFSI-5 blends where these systems exhibit maximums in σ_r at similar values of *r,* due to the chemical similarities. However, the PEO-based system has a significantly higher value of σ_r compared to the POEM-based system at all compositions. This is likely due to the differences in the ion solvation structure of the EO-containing polymers, as it is known that the EO's closest to the backbone in POEM do not readily participate in ion transport.[107] Therefore, the lower value of σ_r for the POEM-based systems indicates that the differences in ionic conductivity observed are due to a less-coordinated ion solvation environment within POEM versus PEO. Similar to the PEO/P2/LiX blends, the solvation site quality can be tuned, but the addition of the charge carriers decreases the segmental motion. Unlike the ternary systems, the blend composition of the SICPBs is directly tied to the quantity of lithium ions, making the optimization of these systems, i.e., the balance between segmental motion and ion solvation structure, challenging.

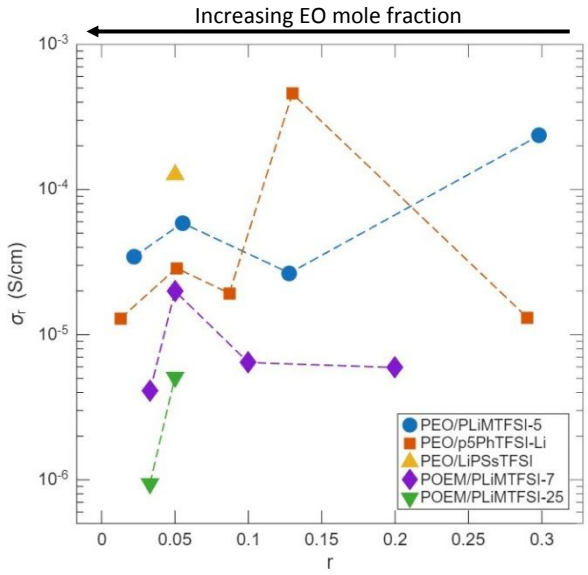

Figure 9. Reduced conductivity, σ_r, as a function of salt concentration, r, for the single-ion conducting polymer blends. σ_r was evaluated at $T = T_g + 100$ for all blends.

Conclusions and Outlook

In this work, we deconvolute the primary factors affecting observed differences in ionic conductivity in PEO-based PBEs to guide the design of electrolytes with improved performance. Our analysis utilizes reduced conductivity as a metric to isolate the effect of polymer segmental motion on ion transport from other contributing factors, such as the ion solvation environment. We found that for PEO blends doped with $LiClO_4$, segmental motion is the primary driver behind the difference in ionic conductivity, particularly below a 0.95 EO mole fraction. This indicates that

View Article Online
DOI: 10.1039/D6LP00078A

tuning $T_{g,blend}$ is the main lever to enhance ion transport in these systems at specific salt concentrations. In contrast, blends prepared with LiTFSI show a broader range of σ_r values, indicating that the ion solvation environment plays a bigger role in the ionic conductivity than in $LiClO_4$ systems. While T_g remains important, these findings imply that T_g-independent factors can be leveraged to engineer the ion solvation environment to improve ion transport in LiTFSI-based PBEs. SICPB systems are more complex, as the blend composition is intrinsically linked to the Li^+ ion concentration. We observe that maximum ionic conductivity occurs at intermediate salt concentrations, reflecting a complex balance between the number of charge carriers and segmental motion. Notably, some SICPB systems exhibited decoupled ion transport, where ion transport properties were less affected by changes in blend composition. Ultimately, our analysis shows that ion solvation and distribution have a larger impact on performance than the number of charge carriers alone in SICPBs. To summarize our findings, while polymer segmental motion appears to be a universal factor, the relative importance of other factors, such as the ion solvation environment, changes between $LiClO_4$, LiTFSI, and SICPB systems. Deconvoluting these complex interconnected factors is essential to gaining a deeper understanding of the behavior in these systems and for guiding the rational design of next-generation polymer electrolytes.

Based on these findings, we recommend that other researchers studying PBEs consider including a range of temperature dependent ionic conductivity data as well as all thermal transitions of each sample when reporting their findings. Though ion transport and segmental motion are often correlated, the true relationship cannot be fully understood without both datasets, as we have demonstrated here. Additionally, providing this data would enable direct comparisons within the literature in order to provide a deeper understanding into how ion transport can be tuned by segmental dynamics and ion solvation environment. However, metrics such as reduced conductivity have limits in their usefulness as it cannot individually describe the individual effect of electrolyte properties, such as polymer structure, ion dissociation, and solvation site connecteness, on ion transport. Gaining a deeper understanding into the impact of each individual property is critical to designing an electrolyte with high ionic conductivity and desirable mechanical properties for applications in next-generation LMBs. While PBEs tend to achieve higher ionic conductivities, the tie to segmental motion often results in liquid-like behavior, which can limit their maximum rate of ion transport. While SICPBs often display more robust mechanical properties and electrochemical performance, the ionic conductivity is often limited due to reduced segmental motion. Therefore, the primary route of improvement is the decoupling of ion transport from segmental motion such that the mechanical properties and ion motion can be tuned independently to generate electrolytes with optimized performance.

Nomenclature:

A	Pre-exponential factor
DSC	Differential scanning calorimetry
E_a	Pseudo activation energy (kJ/mol)
EO	Ethylene oxide
k	Kwei fitting parameter 1

View Article Online
DOI: 10.1039/D6LP00078A

k_B	Boltzmann constant (J/K)
LIB	Lithium-ion battery
$LiClO_4$	Lithium perchlorate
LiPSsTFSI	Poly[(4-styrenesulfonyl)(trifluoromethyl(S-trifluoromethylsulfonylimino)sulfonyl)imide]
LiTFSI	Lithium bis(trifluoromethanesulfonyl)imide
LMB	Lithium metal batteries
M_e	Entanglement molecular weight (kDa)
$M_{n,P2}$	Molecular weight of polymer 2 (kDa)
$M_{n,PEO}$	Molecular weight of PEO (kDa)
N_i	Characterizes chain length of polymer i
P(2EO-MO)	poly(1,3,6-trioxocane)
P2VP	Poly(2-vinylpyridine)
P4VP	Poly(4-vinylpyridine)
P5PhTFSI-Li	Phenylsulfonyl (trifluoromethylsulfonyl)imide-lithium
PBE	Polymer blend electrolyte
PDTOA	Poly(dithiooxamide)
PEI	Polyethylenimine
PEO	Poly(ethylene oxide)
PES	Poly(oligo[oxyethylene]oxysebacoyl)
PFPE	Perfluoropolyether
PLiMTFSI	Poly[lithium sulfonyl (trifluoromethane sulfonyl)imidemethacrylate]
PMMA	Poly(methyl methacrylate)
POEM	poly(oligo ethylene oxide methacrylate)
q	Kwei fitting parameter 2
r	$[Li^+]/[EO]$
R	Universal gas constant (J/mol K)
SICPB	Single-ion conducting polymer blend
SICPE	Single-ion conducting polymer electrolyte
SSE	Solid state electrolyte
T	Temperature (K)
T_0	Vogel temperature (K)
T_g	Glass transition temperature (°C)
$T_{g,blend}$	Glass transition temperature of the polymer blend
t_{Li+}	Li^+ transference number
T_m	Melting temperature (°C)
VTF	Vogel-Fulcher-Tamman
w_i	Weight fraction of component i
w_{PEO}	PEO weight fraction
ΔG_{mix}	Gibbs free energy of mixing (J)
σ	Ionic conductivity (S/cm)
σ_r	Reduced conductivity (S/cm)
ϕ_i	Volume fraction of component i
χ	Flory-Huggins interaction parameter
χ_{eff}	Effective interaction parameter

View Article Online
DOI: 10.1039/D6LP00078A

Author Contributions

Marissa Gallmeyer: conceptualization, data curation, formal analysis, investigation, methodology, validation, visualization, writing—original draft

Thorfinnur A. H. Baldvinsson: conceptualization, data curation, formal analysis, investigation, methodology, validation, visualization, writing—original draft

Whitney S Loo: conceptualization, funding acquisition, methodology, project administration, resources, supervision, writing—review & editing

Conflict of Interest

There are no conflicts to declare.

Data Availability

All glass transition temperature data and corresponding fits and results from fitting ionic conductivity data are available in the Supplemental Information.

Acknowledgements

This research was primarily supported by NSF through the University of Wisconsin Materials Research Science and Engineering Center (DMR-2309000).

References

(1) Barton, J. P.; Infield, D. G. Energy Storage and Its Use with Intermittent Renewable Energy. *IEEE Transactions on Energy Conversion* **2004**, *19* (2), 441–448. https://doi.org/10.1109/TEC.2003.822305.
(2) Denholm, P.; Ela, E.; Kirby, B.; Milligan, M. The Role of Energy Storage with Renewable Electricity Generation. **2010**. https://doi.org/10.2172/972169.
(3) Goodenough, J. B.; Park, K.-S. The Li-Ion Rechargeable Battery: A Perspective. *J. Am. Chem. Soc.* **2013**, *135* (4), 1167–1176. https://doi.org/10.1021/ja3091438.
(4) Choi, J. W.; Aurbach, D. Promise and Reality of Post-Lithium-Ion Batteries with High Energy Densities. *Nat Rev Mater* **2016**, *1* (4), 16013. https://doi.org/10.1038/natrevmats.2016.13.
(5) Thackeray, M. M.; Wolverton, C.; Isaacs, E. D. Electrical Energy Storage for Transportation—Approaching the Limits of, and Going beyond, Lithium-Ion Batteries. *Energy Environ. Sci.* **2012**, *5* (7), 7854–7863. https://doi.org/10.1039/C2EE21892E.
(6) Tarascon, J.-M.; Armand, M. Issues and Challenges Facing Rechargeable Lithium Batteries. *Nature* **2001**, *414* (6861), 359–367. https://doi.org/10.1038/35104644.
(7) Boyer, E. The Lithium-Ion (EV) Battery Market and Supply Chain.
(8) Qian, J.; Henderson, W. A.; Xu, W.; Bhattacharya, P.; Engelhard, M.; Borodin, O.; Zhang, J.-G. High Rate and Stable Cycling of Lithium Metal Anode. *Nat Commun* **2015**, *6* (1), 6362. https://doi.org/10.1038/ncomms7362.
(9) Xu, W.; Wang, J.; Ding, F.; Chen, X.; Nasybulin, E.; Zhang, Y.; Zhang, J.-G. Lithium Metal Anodes for Rechargeable Batteries. *Energy Environ. Sci.* **2014**, *7* (2), 513–537. https://doi.org/10.1039/C3EE40795K.

View Article Online
DOI: 10.1039/D6LP00078A

(10) Goodenough, J. B.; Kim, Y. Challenges for Rechargeable Li Batteries. *Chem. Mater.* **2010**, *22* (3), 587–603. https://doi.org/10.1021/cm901452z.
(11) Vogdanis, L.; Martens, B.; Uchtmann, H.; Hensel, F.; Heitz, W. Synthetic and Thermodynamic Investigations in the Polymerization of Ethylene Carbonate. *Die Makromolekulare Chemie* **1990**, *191* (3), 465–472. https://doi.org/10.1002/macp.1990.021910301.
(12) Lin, D.; Liu, Y.; Cui, Y. Reviving the Lithium Metal Anode for High-Energy Batteries. *Nature Nanotech* **2017**, *12* (3), 194–206. https://doi.org/10.1038/nnano.2017.16.
(13) Varzi, A.; Thanner, K.; Scipioni, R.; Di Lecce, D.; Hassoun, J.; Dörfler, S.; Altheus, H.; Kaskel, S.; Prehal, C.; Freunberger, S. A. Current Status and Future Perspectives of Lithium Metal Batteries. *Journal of Power Sources* **2020**, *480*, 228803. https://doi.org/10.1016/j.jpowsour.2020.228803.
(14) Wang, J.; Ge, B.; Li, H.; Yang, M.; Wang, J.; Liu, D.; Fernandez, C.; Chen, X.; Peng, Q. Challenges and Progresses of Lithium-Metal Batteries. *Chemical Engineering Journal* **2021**, *420*, 129739. https://doi.org/10.1016/j.cej.2021.129739.
(15) Cohen, Y. S.; Cohen, Y.; Aurbach, D. Micromorphological Studies of Lithium Electrodes in Alkyl Carbonate Solutions Using in Situ Atomic Force Microscopy. *J. Phys. Chem. B* **2000**, *104* (51), 12282–12291. https://doi.org/10.1021/jp002526b.
(16) Armand, M.; Tarascon, J.-M. Building Better Batteries. *Nature* **2008**, *451* (7179), 652–657. https://doi.org/10.1038/451652a.
(17) Kim, H.; Jeong, G.; Kim, Y.-U.; Kim, J.-H.; Park, C.-M.; Sohn, H.-J. Metallic Anodes for next Generation Secondary Batteries. *Chem. Soc. Rev.* **2013**, *42* (23), 9011–9034. https://doi.org/10.1039/C3CS60177C.
(18) Yang, C.; Fu, K.; Zhang, Y.; Hitz, E.; Hu, L. Protected Lithium-Metal Anodes in Batteries: From Liquid to Solid. *Advanced Materials* **2017**, *29* (36), 1701169. https://doi.org/10.1002/adma.201701169.
(19) Banerjee, A.; Wang, X.; Fang, C.; Wu, E. A.; Meng, Y. S. Interfaces and Interphases in All-Solid-State Batteries with Inorganic Solid Electrolytes. *Chem. Rev.* **2020**, *120* (14), 6878–6933. https://doi.org/10.1021/acs.chemrev.0c00101.
(20) Knauth, P.; Tuller, H. L. Solid-State Ionics: Roots, Status, and Future Prospects. *Journal of the American Ceramic Society* **2002**, *85* (7), 1654–1680. https://doi.org/10.1111/j.1151-2916.2002.tb00334.x.
(21) Quartarone, E.; Mustarelli, P. Electrolytes for Solid-State Lithium Rechargeable Batteries: Recent Advances and Perspectives. *Chem. Soc. Rev.* **2011**, *40* (5), 2525–2540. https://doi.org/10.1039/C0CS00081G.
(22) Hu, Y.-S. Batteries: Getting Solid. *Nat Energy* **2016**, *1* (4), 16042. https://doi.org/10.1038/nenergy.2016.42.
(23) Armand, M. Polymer Solid Electrolytes - an Overview. *Solid State Ionics* **1983**, *9–10*, 745–754. https://doi.org/10.1016/0167-2738(83)90083-8.
(24) Varzi, A.; Raccichini, R.; Passerini, S.; Scrosati, B. Challenges and Prospects of the Role of Solid Electrolytes in the Revitalization of Lithium Metal Batteries. *J. Mater. Chem. A* **2016**, *4* (44), 17251–17259. https://doi.org/10.1039/C6TA07384K.
(25) Zhang, D.; Li, L.; Wu, X.; Wang, J.; Li, Q.; Pan, K.; He, J. Research Progress and Application of PEO-Based Solid State Polymer Composite Electrolytes. *Front. Energy Res.* **2021**, *9*. https://doi.org/10.3389/fenrg.2021.726738.
(26) Xue, Z.; He, D.; Xie, X. Poly(Ethylene Oxide)-Based Electrolytes for Lithium-Ion Batteries. *J. Mater. Chem. A* **2015**, *3* (38), 19218–19253. https://doi.org/10.1039/C5TA03471J.
(27) Fenton, D. E.; Parker, J. M.; Wright, P. V. Complexes of Alkali Metal Ions with Poly(Ethylene Oxide). *Polymer* **1973**, *14* (11), 589. https://doi.org/10.1016/0032-3861(73)90146-8.
(28) Tominaga, Y.; Shimomura, T.; Nakamura, M. Alternating Copolymers of Carbon Dioxide with Glycidyl Ethers for Novel Ion-Conductive Polymer Electrolytes. *Polymer* **2010**, *51* (19), 4295–4298. https://doi.org/10.1016/j.polymer.2010.07.037.

View Article Online
DOI: 10.1039/D6LP00078A

(29) Wong, D. H. C.; Thelen, J. L.; Fu, Y.; Devaux, D.; Pandya, A. A.; Battaglia, V. S.; Balsara, N. P.; DeSimone, J. M. Nonflammable Perfluoropolyether-Based Electrolytes for Lithium Batteries. *Proceedings of the National Academy of Sciences* **2014**, *111* (9), 3327–3331. https://doi.org/10.1073/pnas.1314615111.
(30) Blonsky, P. M.; Shriver, D. F.; Austin, P.; Allcock, H. R. Complex Formation and Ionic Conductivity of Polyphosphazene Solid Electrolytes. *Solid State Ionics* **1986**, *18–19*, 258–264. https://doi.org/10.1016/0167-2738(86)90123-2.
(31) Long, L.; Wang, S.; Xiao, M.; Meng, Y. Polymer Electrolytes for Lithium Polymer Batteries. *J. Mater. Chem. A* **2016**, *4* (26), 10038–10069. https://doi.org/10.1039/C6TA02621D.
(32) Lascaud, S.; Perrier, M.; Vallee, A.; Besner, S.; Prud'homme, J.; Armand, M. Phase Diagrams and Conductivity Behavior of Poly(Ethylene Oxide)-Molten Salt Rubbery Electrolytes. *Macromolecules* **1994**, *27* (25), 7469–7477. https://doi.org/10.1021/ma00103a034.
(33) Grundy, L. S.; Fu, S.; Hoffman, Z. J.; Balsara, N. P. Electrochemical Characterization of PEO/LiTFSI Electrolytes Near the Solubility Limit. *Macromolecules* **2022**, *55* (20), 9030–9038. https://doi.org/10.1021/acs.macromol.2c01655.
(34) Yang, H.; Wu, N. Ionic Conductivity and Ion Transport Mechanisms of Solid-State Lithium-Ion Battery Electrolytes: A Review. *Energy Science & Engineering* **2022**, *10* (5), 1643–1671. https://doi.org/10.1002/ese3.1163.
(35) Hallinan, D. T.; Balsara, N. P. Polymer Electrolytes. *Annu. Rev. Mater. Res.* **2013**, *43* (1), 503–525. https://doi.org/10.1146/annurev-matsci-071312-121705.
(36) Mauger, A.; Julien, C. M.; Paolella, A.; Armand, M.; Zaghib, K. Building Better Batteries in the Solid State: A Review. *Materials* **2019**, *12* (23), 3892. https://doi.org/10.3390/ma12233892.
(37) Das, S.; Ghosh, A. Effect of Plasticizers on Ionic Conductivity and Dielectric Relaxation of PEO-LiClO4 Polymer Electrolyte. *Electrochimica Acta* **2015**, *171*, 59–65. https://doi.org/10.1016/j.electacta.2015.04.178.
(38) Meng, N.; Ye, Y.; Yang, Z.; Li, H.; Lian, F. Developing Single-Ion Conductive Polymer Electrolytes for High-Energy-Density Solid State Batteries. *Advanced Functional Materials* **2023**, *33* (43), 2305072. https://doi.org/10.1002/adfm.202305072.
(39) Meyer, W. H. Polymer Electrolytes for Lithium-Ion Batteries. *Advanced Materials* **1998**, *10* (6), 439–448. https://doi.org/10.1002/(SICI)1521-4095(199804)10:6%3C439::AID-ADMA439%3E3.0.CO;2-I.
(40) Mao, G.; Saboungi, M.-L.; Price, D. L.; Armand, M. B.; Howells, W. S. Structure of Liquid PEO-LiTFSI Electrolyte. *Phys. Rev. Lett.* **2000**, *84* (24), 5536–5539. https://doi.org/10.1103/PhysRevLett.84.5536.
(41) Bennington, P.; Deng, C.; Sharon, D.; Webb, M. A.; Pablo, J. J. de; Nealey, P. F.; Patel, S. N. Role of Solvation Site Segmental Dynamics on Ion Transport in Ethylene-Oxide Based Side-Chain Polymer Electrolytes. *J. Mater. Chem. A* **2021**, *9* (15), 9937–9951. https://doi.org/10.1039/D1TA00899D.
(42) Borodin, O.; Smith, G. D. Mechanism of Ion Transport in Amorphous Poly(Ethylene Oxide)/LiTFSI from Molecular Dynamics Simulations. *Macromolecules* **2006**, *39* (4), 1620–1629. https://doi.org/10.1021/ma052277v.
(43) Bresser, D.; Lyonnard, S.; Iojoiu, C.; Picard, L.; Passerini, S. Decoupling Segmental Relaxation and Ionic Conductivity for Lithium-Ion Polymer Electrolytes. *Mol. Syst. Des. Eng.* **2019**, *4* (4), 779–792. https://doi.org/10.1039/C9ME00038K.
(44) Marzantowicz, M.; Krok, F.; Dygas, J. R.; Florjańczyk, Z.; Zygadło-Monikowska, E. The Influence of Phase Segregation on Properties of Semicrystalline PEO:LiTFSI Electrolytes. *Solid State Ionics* **2008**, *179* (27), 1670–1678. https://doi.org/10.1016/j.ssi.2007.11.035.
(45) Cheng, S.; Smith, D. M.; Li, C. Y. How Does Nanoscale Crystalline Structure Affect Ion Transport in Solid Polymer Electrolytes? *Macromolecules* **2014**, *47* (12), 3978–3986. https://doi.org/10.1021/ma500734q.
(46) Ratner, M. A.; Johansson, P.; Shriver, D. F. Polymer Electrolytes: Ionic Transport Mechanisms and Relaxation Coupling. *MRS Bulletin* **2000**, *25* (3), 31–37. https://doi.org/10.1557/mrs2000.16.

View Article Online
DOI: 10.1039/D6LP00078A

(47) Gudla, H.; Hockmann, A.; Brandell, D.; Mindemark, J. To Hop or Not to Hop: Unveiling Different Modes of Ion Transport in Solid Polymer Electrolytes through Molecular Dynamics Simulations. *ACS Appl Polym Mater* **2025**, *7* (8), 4716–4724. https://doi.org/10.1021/acsapm.4c03724.

(48) Aziz, S. B.; Woo, T. J.; Kadir, M. F. Z.; Ahmed, H. M. A Conceptual Review on Polymer Electrolytes and Ion Transport Models. *Journal of Science: Advanced Materials and Devices* **2018**, *3* (1), 1–17. https://doi.org/10.1016/j.jsamd.2018.01.002.

(49) Ghelichi, M.; Qazvini, N. T.; Jafari, S. H.; Khonakdar, H. A.; Farajollahi, Y.; Scheffler, C. Conformational, Thermal, and Ionic Conductivity Behavior of PEO in PEO/PMMA Miscible Blend: Investigating the Effect of Lithium Salt. *Journal of Applied Polymer Science* **2013**, *129* (4), 1868–1874. https://doi.org/10.1002/app.38897.

(50) Zhang, C.; Gamble, S.; Ainsworth, D.; Slawin, A. M. Z.; Andreev, Y. G.; Bruce, P. G. Alkali Metal Crystalline Polymer Electrolytes. *Nature Mater* **2009**, *8* (7), 580–584. https://doi.org/10.1038/nmat2474.

(51) Petrowsky, M.; Frech, R. Temperature Dependence of Ion Transport: The Compensated Arrhenius Equation. *J. Phys. Chem. B* **2009**, *113* (17), 5996–6000. https://doi.org/10.1021/jp810095g.

(52) Jones, S. D.; Bamford, J.; Fredrickson, G. H.; Segalman, R. A. Decoupling Ion Transport and Matrix Dynamics to Make High Performance Solid Polymer Electrolytes. *ACS Polym. Au* **2022**, *2* (6), 430–448. https://doi.org/10.1021/acspolymersau.2c00024.

(53) Wang, Y.; Fan, F.; Agapov, A. L.; Yu, X.; Hong, K.; Mays, J.; Sokolov, A. P. Design of Superionic Polymers—New Insights from Walden Plot Analysis. *Solid State Ionics* **2014**, *262*, 782–784. https://doi.org/10.1016/j.ssi.2013.09.026.

(54) Wang, Y.; Fan, F.; Agapov, A. L.; Saito, T.; Yang, J.; Yu, X.; Hong, K.; Mays, J.; Sokolov, A. P. Examination of the Fundamental Relation between Ionic Transport and Segmental Relaxation in Polymer Electrolytes. *Polymer* **2014**, *55* (16), 4067–4076. https://doi.org/10.1016/j.polymer.2014.06.085.

(55) Paren, B. A.; Nguyen, N.; Ballance, V.; Hallinan, D. T.; Kennemur, J. G.; Winey, K. I. Superionic Li-Ion Transport in a Single-Ion Conducting Polymer Blend Electrolyte. *Macromolecules* **2022**, *55* (11), 4692–4702. https://doi.org/10.1021/acs.macromol.2c00459.

(56) Wood, B. C.; Varley, J. B.; Kweon, K. E.; Shea, P.; Hall, A. T.; Grieder, A.; Ward, M.; Aguirre, V. P.; Rigling, D.; Lopez Ventura, E.; Stancill, C.; Adelstein, N. Paradigms of Frustration in Superionic Solid Electrolytes. *Philos Trans A Math Phys Eng Sci 379* (2211), 20190467. https://doi.org/10.1098/rsta.2019.0467.

(57) Hull, S. Superionics: Crystal Structures and Conduction Processes. *Rep. Prog. Phys.* **2004**, *67* (7), 1233. https://doi.org/10.1088/0034-4885/67/7/R05.

(58) Devkota, G. P.; Dauenhauer, C. K.; Jiang, J.; Schaefer, J. L. Structure and Dynamics in Poly(Ethylene Oxide)-Blended Single-Ion Conducting Polymer Electrolytes Based on Side-Chain Ionomers. *Polym. Chem.* **2025**, *16* (47), 5106–5115. https://doi.org/10.1039/D5PY00769K.

(59) Jones, S. D.; Nguyen, H.; Richardson, P. M.; Chen, Y.-Q.; Wyckoff, K. E.; Hawker, C. J.; Clément, R. J.; Fredrickson, G. H.; Segalman, R. A. Design of Polymeric Zwitterionic Solid Electrolytes with Superionic Lithium Transport. *ACS Cent. Sci.* **2022**, *8* (2), 169–175. https://doi.org/10.1021/acscentsci.1c01260.

(60) Yang, M.; Epps, T. H. Superionic Conduction in Solid Polymer Electrolytes – Decoupling Ion Transport from Segmental Relaxation. *Polym. Chem.* **2026**, *17* (10), 971–983. https://doi.org/10.1039/D5PY01070E.

(61) Pesko, D. M.; Jung, Y.; Hasan, A. L.; Webb, M. A.; Coates, G. W.; Miller, T. F.; Balsara, N. P. Effect of Monomer Structure on Ionic Conductivity in a Systematic Set of Polyester Electrolytes. *Solid State Ionics* **2016**, *289*, 118–124. https://doi.org/10.1016/j.ssi.2016.02.020.

(62) Pesko, D. M.; Webb, M. A.; Jung, Y.; Zheng, Q.; Miller, T. F. I.; Coates, G. W.; Balsara, N. P. Universal Relationship between Conductivity and Solvation-Site Connectivity in Ether-Based Polymer Electrolytes. *Macromolecules* **2016**, *49* (14), 5244–5255. https://doi.org/10.1021/acs.macromol.6b00851.

View Article Online
DOI: 10.1039/D6LP00078A

(63) Zheng, Q.; Pesko, D. M.; Savoie, B. M.; Timachova, K.; Hasan, A. L.; Smith, M. C.; Miller, T. F. I.; Coates, G. W.; Balsara, N. P. Optimizing Ion Transport in Polyether-Based Electrolytes for Lithium Batteries. *Macromolecules* **2018**, *51* (8), 2847–2858. https://doi.org/10.1021/acs.macromol.7b02706.
(64) Gudla, H.; Zhang, C.; Brandell, D. Effects of Solvent Polarity on Li-Ion Diffusion in Polymer Electrolytes: An All-Atom Molecular Dynamics Study with Charge Scaling. *J. Phys. Chem. B* **2020**, *124* (37), 8124–8131. https://doi.org/10.1021/acs.jpcb.0c05108.
(65) Blatt, M. P.; Hallinan, D. T. Jr. Polymer Blend Electrolytes for Batteries and Beyond. *Ind. Eng. Chem. Res.* **2021**, *60* (48), 17303–17327. https://doi.org/10.1021/acs.iecr.1c02938.
(66) Knychała, P.; Timachova, K.; Banaszak, M.; Balsara, N. P. 50th Anniversary Perspective: Phase Behavior of Polymer Solutions and Blends. *Macromolecules* **2017**, *50* (8), 3051–3065. https://doi.org/10.1021/acs.macromol.6b02619.
(67) Hiemenz, P. C.; Lodge, T. P. *Polymer Chemistry*, 2nd ed.; CRC Press, 2007.
(68) Kim, J. H.; Min, B. R.; Kang, Y. S. Thermodynamic Model of the Glass Transition Behavior for Miscible Polymer Blends. *Macromolecules* **2006**, *39* (3), 1297–1299. https://doi.org/10.1021/ma052436a.
(69) Lodge, T. P.; Wood, E. R.; Haley, J. C. Two Calorimetric Glass Transitions Do Not Necessarily Indicate Immiscibility: The Case of PEO/PMMA. *Journal of Polymer Science Part B: Polymer Physics* **2006**, *44* (4), 756–763. https://doi.org/10.1002/polb.20735.
(70) Gao, K. W.; Loo, W. S.; Snyder, R. L.; Abel, B. A.; Choo, Y.; Lee, A.; Teixeira, S. C. M.; Garetz, B. A.; Coates, G. W.; Balsara, N. P. Miscible Polyether/Poly(Ether–Acetal) Electrolyte Blends. *Macromolecules* **2020**, *53* (14), 5728–5739. https://doi.org/10.1021/acs.macromol.0c00747.
(71) He, Y.; Lutz, T. R.; Ediger, M. D. Segmental and Terminal Dynamics in Miscible Polymer Mixtures: Tests of the Lodge–McLeish Model. *The Journal of Chemical Physics* **2003**, *119* (18), 9956–9965. https://doi.org/10.1063/1.1615963.
(72) Lodge, T. P.; McLeish, T. C. B. Self-Concentrations and Effective Glass Transition Temperatures in Polymer Blends. *Macromolecules* **2000**, *33* (14), 5278–5284. https://doi.org/10.1021/ma9921706.
(73) Zhu, C.; Pedretti, B. J.; Kuehster, L.; Ganesan, V.; Sanoja, G. E.; Lynd, N. A. Ionic Conductivity, Salt Partitioning, and Phase Separation in High-Dielectric Contrast Polyether Blends and Block Polymer Electrolytes. *Macromolecules* **2023**, *56* (3), 1086–1096. https://doi.org/10.1021/acs.macromol.2c02023.
(74) Pryamitsyn, V. A.; Kwon, H.-K.; Zwanikken, J. W.; Olvera de la Cruz, M. Anomalous Phase Behavior of Ionic Polymer Blends and Ionic Copolymers. *Macromolecules* **2017**, *50* (13), 5194–5207. https://doi.org/10.1021/acs.macromol.7b00523.
(75) Sing, C. E.; Olvera de la Cruz, M. Polyelectrolyte Blends and Nontrivial Behavior in Effective Flory–Huggins Parameters. *ACS Macro Lett.* **2014**, *3* (8), 698–702. https://doi.org/10.1021/mz500202n.
(76) Bakar, R.; Darvishi, S.; Li, T.; Han, M.; Aydemir, U.; Nizamoglu, S.; Hong, K.; Senses, E. Effect of Polymer Topology on Microstructure, Segmental Dynamics, and Ionic Conductivity in PEO/PMMA-Based Solid Polymer Electrolytes. *ACS Appl. Polym. Mater.* **2022**, *4* (1), 179–190. https://doi.org/10.1021/acsapm.1c01178.
(77) Shah, N. J.; Shalaby, M.; He, L.; Wang, X.; Deslandes, D.; Garetz, B. A.; Balsara, N. P. Chimney-Shaped Phase Diagram in a Polymer Blend Electrolyte. *ACS Macro Lett.* **2023**, 874–879. https://doi.org/10.1021/acsmacrolett.3c00285.
(78) Sharon, D.; Deng, C.; Bennington, P.; Webb, M. A.; Patel, S. N.; de Pablo, J. J.; Nealey, P. F. Critical Percolation Threshold for Solvation-Site Connectivity in Polymer Electrolyte Mixtures. *Macromolecules* **2022**, *55* (16), 7212–7221. https://doi.org/10.1021/acs.macromol.2c00988.
(79) Shah, N. J.; He, L.; Gao, K. W.; Balsara, N. P. Thermodynamics and Phase Behavior of Poly(Ethylene Oxide)/Poly(Methyl Methacrylate)/Salt Blend Electrolytes Studied by Small-Angle Neutron Scattering. *Macromolecules* **2023**, *56* (7), 2889–2898. https://doi.org/10.1021/acs.macromol.2c02533.

View Article Online
DOI: 10.1039/D6LP00078A

(80) Gallmeyer, M.; Wu, H.-J.; Breining, W.; Lynn, D. M.; Loo, W. S. Thermal Properties and Ionic Conductivity in Salt-Containing POEM/PEO Polymer Blend Electrolytes. *ACS Appl. Polym. Mater.* **2025**. https://doi.org/10.1021/acsapm.5c01118.
(81) Zhang, H.; Li, C.; Piszcz, M.; Coya, E.; Rojo, T.; Rodriguez-Martinez, L. M.; Armand, M.; Zhou, Z. Single Lithium-Ion Conducting Solid Polymer Electrolytes: Advances and Perspectives. *Chem. Soc. Rev.* **2017**, *46* (3), 797–815. https://doi.org/10.1039/C6CS00491A.
(82) Sun, X.-G.; Kerr, J. B. Synthesis and Characterization of Network Single Ion Conductors Based on Comb-Branched Polyepoxide Ethers and Lithium Bis(Allylmalonato)Borate. *Macromolecules* **2006**, *39* (1), 362–372. https://doi.org/10.1021/ma0507701.
(83) Huo, S.; Sheng, L.; Xue, W.; Wang, L.; Xu, H.; Zhang, H.; He, X. Challenges of Polymer Electrolyte with Wide Electrochemical Window for High Energy Solid-State Lithium Batteries. *InfoMat* **2023**, *5* (3), e12394. https://doi.org/10.1002/inf2.12394.
(84) Stolz, L.; Hochstädt, S.; Röser, S.; Hansen, M. R.; Winter, M.; Kasnatscheew, J. Single-Ion versus Dual-Ion Conducting Electrolytes: The Relevance of Concentration Polarization in Solid-State Batteries. *ACS Appl. Mater. Interfaces* **2022**, *14* (9), 11559–11566. https://doi.org/10.1021/acsami.2c00084.
(85) Hoffman, Z. J.; Ho, A. S.; Chakraborty, S.; Balsara, N. P. Limiting Current Density in Single-Ion-Conducting and Conventional Block Copolymer Electrolytes. *J. Electrochem. Soc.* **2022**, *169* (4), 043502. https://doi.org/10.1149/1945-7111/ac613b.
(86) Bannister, D. J.; Davies, G. R.; Ward, I. M.; McIntyre, J. E. Ionic Conductivities for Poly(Ethylene Oxide) Complexes with Lithium Salts of Monobasic and Dibasic Acids and Blends of Poly(Ethylene Oxide) with Lithium Salts of Anionic Polymers. *Polymer* **1984**, *25* (9), 1291–1296. https://doi.org/10.1016/0032-3861(84)90378-1.
(87) Diederichsen, K. M.; McShane, E. J.; McCloskey, B. D. Promising Routes to a High Li+ Transference Number Electrolyte for Lithium Ion Batteries. *ACS Energy Lett.* **2017**, *2* (11), 2563–2575. https://doi.org/10.1021/acsenergylett.7b00792.
(88) Olmedo-Martínez, J. L.; Porcarelli, L.; Alegría, Á.; Mecerreyes, D.; Müller, A. J. High Lithium Conductivity of Miscible Poly(Ethylene Oxide)/Methacrylic Sulfonamide Anionic Polyelectrolyte Polymer Blends. *Macromolecules* **2020**, *53* (11), 4442–4453. https://doi.org/10.1021/acs.macromol.0c00703.
(89) Zhu, J.; Zhang, Z.; Zhao, S.; Westover, A. S.; Belharouak, I.; Cao, P.-F. Single-Ion Conducting Polymer Electrolytes for Solid-State Lithium–Metal Batteries: Design, Performance, and Challenges. *Advanced Energy Materials* **2021**, *11* (14), 2003836. https://doi.org/10.1002/aenm.202003836.
(90) Yang, M.; Epps, T. H. I. Solid-State, Single-Ion Conducting, Polymer Blend Electrolytes with Enhanced Li+ Conduction, Electrochemical Stability, and Limiting Current Density. *Chem. Mater.* **2024**, *36* (4), 1855–1869. https://doi.org/10.1021/acs.chemmater.3c02389.
(91) Blatt, M. P.; Hallinan, D. T. Jr. Polymer Blend Electrolytes for Batteries and Beyond. *Ind. Eng. Chem. Res.* **2021**, *60* (48), 17303–17327. https://doi.org/10.1021/acs.iecr.1c02938.
(92) Schauser, N. S.; Seshadri, R.; Segalman, R. A. Multivalent Ion Conduction in Solid Polymer Systems. *Mol. Syst. Des. Eng.* **2019**, *4* (2), 263–279. https://doi.org/10.1039/C8ME00096D.
(93) Kwei, T. K. The Effect of Hydrogen Bonding on the Glass Transition Temperatures of Polymer Mixtures. *Journal of Polymer Science: Polymer Letters Edition* **1984**, *22* (6), 307–313. https://doi.org/10.1002/pol.1984.130220603.
(94) Anshyang, L. A.; Kwei, T. K.; Reiser, A. On the Physical Meaning of the Kwei Equation for the Glass Transition of Polymer Blends. *Macromolecules* **1989**, *22* (10).
(95) Gordon, M.; Taylor, J. S. Ideal Copolymers and the Second-Order Transitions of Synthetic Rubbers. i. Non-Crystalline Copolymers. *Journal of Applied Chemistry* **1952**, *2* (9), 493–500. https://doi.org/10.1002/jctb.5010020901.
(96) Schneider, H. A. Glass Transition Behaviour of Compatible Polymer Blends. *Polymer* **1989**, *30* (5), 771–779. https://doi.org/10.1016/0032-3861(89)90172-9.

View Article Online
DOI: 10.1039/D6LP00078A

(97) Fox, G. T. Influence of Diluent and of Copolymer Com- Position on the Glass Temperature of a Polymer System. *Bulletin of the American Physical Society* **1956**, *1*.
(98) Tanaka, R.; Sakurai, M.; Sekiguchi, H.; Mori, H.; Murayama, T.; Ooyama, T. Lithium Ion Conductivity in Polyoxyethylene/Polyethylenimine Blends. *Electrochimica Acta* **2001**, *46* (10), 1709–1715. https://doi.org/10.1016/S0013-4686(00)00775-1.
(99) Sim, J. H.; Hong, W.; Vu, T. V.; Choi, H.; Kim, J.; Lee, Y.; Kang, Y. Unlocking Hidden Miscibility: Entropy Diluent Strategy for Incompatible Polymer Blends. *Macromolecules* **2025**, *58* (18), 9682–9691. https://doi.org/10.1021/acs.macromol.5c01387.
(100) Kim, D.-W.; Park, J.-K.; Rhee, H.-W. Conductivity and Thermal Studies of Solid Polymer Electrolytes Prepared by Blending Poly(Ethylene Oxide), Poly(Oligo[Oxyethylene]Oxysebacoyl) and Lithium Perchlorate. *Solid State Ionics* **1996**, *83* (1), 49–56. https://doi.org/10.1016/0167-2738(95)00238-3.
(101) Ghelichi, M.; Qazvini, N. T.; Jafari, S. H.; Khonakdar, H. A.; Farajollahi, Y.; Scheffler, C. Conformational, Thermal, and Ionic Conductivity Behavior of PEO in PEO/PMMA Miscible Blend: Investigating the Effect of Lithium Salt. *Journal of Applied Polymer Science* **2013**, *129* (4), 1868–1874. https://doi.org/10.1002/app.38897.
(102) Li, J.; Khan, I. M. Highly Conductive Solid Polymer Electrolytes Prepared by Blending High Molecular Weight Poly(Ethylene Oxide), Poly(2- or 4-Vinylpyridine), and Lithium Perchlorate. *Macromolecules* **1993**, *26* (17), 4544–4550. https://doi.org/10.1021/ma00069a020.
(103) Gurusiddappa, J.; Madhuri, W.; Padma Suvarna, R.; Priya Dasan, K. Studies on the Morphology and Conductivity of PEO/LiClO4. *Materials Today: Proceedings* **2016**, *3* (6), 1451–1459. https://doi.org/10.1016/j.matpr.2016.04.028.
(104) Banitaba, S. N.; Semnani, D.; Fakhrali, A.; Ebadi, S. V.; Heydari-Soureshjani, E.; Rezaei, B.; Ensafi, A. A. Electrospun PEO Nanofibrous Membrane Enable by LiCl, LiClO4, and LiTFSI Salts: A Versatile Solvent-Free Electrolyte for Lithium-Ion Battery Application. *Ionics* **2020**, *26* (7), 3249–3260. https://doi.org/10.1007/s11581-019-03414-6.
(105) Zhang, J.; Cui, Y.; Zhang, X.; Sun, Q.; Zheng, J.; Wang, P.; Feng, J.; Zhu, Y. LiTFSI as a Plastic Salt in the Quasi-Solid State Polymer Electrolyte for Dye-Sensitized Solar Cells. *Comptes Rendus Chimie* **2013**, *16* (2), 195–200. https://doi.org/10.1016/j.crci.2012.10.015.
(106) Nguyen, N.; Blatt, M. P.; Kim, K.; Hallinan, D. T.; Kennemur, J. G. Investigating Miscibility and Lithium Ion Transport in Blends of Poly(Ethylene Oxide) with a Polyanion Containing Precisely-Spaced Delocalized Charges. *Polym. Chem.* **2022**, *13* (29), 4309–4323. https://doi.org/10.1039/D2PY00605G.
(107) Deng, C.; Webb, M. A.; Bennington, P.; Sharon, D.; Nealey, P. F.; Patel, S. N.; de Pablo, J. J. Role of Molecular Architecture on Ion Transport in Ethylene Oxide-Based Polymer Electrolytes. *Macromolecules* **2021**, *54* (5), 2266–2276. https://doi.org/10.1021/acs.macromol.0c02424.

View Article Online
DOI: 10.1039/D6LP00078A

Perspective: Ion Transport Mechanisms and the Significance of Glass Transition Temperature in PEO based Polymer Blend Electrolytes

Marissa Gallmeyer[a†], Thorfinnur A. H. Baldvinsson[a†], Whitney S. Loo[a*]

[a] University of Wisconsin-Madison Department of Chemical and Biological Engineering, Madison WI, 53706

[†]These authors contributed equally

*Corresponding author email: wloo@wisc.edu

Data Availability

All glass transition temperature data and corresponding fits and results from fitting ionic conductivity data are available in the Supplemental Information.